

# Chapter 1

## The Chemistry of Cold Interstellar Cloud Cores

Eric Herbst

*Department of Physics, The Ohio State University,  
Columbus, OH 43210, USA\**

Tom J. Millar

*Astrophysics Research Centre, School of Mathematics and Physics  
Queen's University Belfast, Belfast BT7 1NN,  
Northern Ireland*

### Contents

1.1	Introduction . . . . .	2
1.1.1	Interstellar Molecules and Their Chemistry . . . . .	4
1.2	Gas-Phase Chemical Processes . . . . .	8
1.2.1	Ion-molecule and Dissociative Recombination Reactions . . . . .	9
1.2.2	Neutral-Neutral Reactions . . . . .	12
1.2.3	Radiative Association . . . . .	13
1.2.4	Organic Chemistry . . . . .	16
1.2.5	Negative Ion Formation . . . . .	19
1.3	Surface Chemistry on Cold Dust Grains: Basic Considerations . . . . .	22
1.3.1	Low-Temperature Surface Chemistry . . . . .	22
1.3.2	H <sub>2</sub> Formation . . . . .	23
1.3.3	Reactions in Ice Mantles . . . . .	24
1.4	Models with Gas-Phase Chemistry . . . . .	25
1.4.1	Time Scales . . . . .	25
1.4.2	Homogeneous Sources . . . . .	26
1.4.3	Non-Homogeneous Sources . . . . .	32
1.5	Deuterium Fractionation . . . . .	35
1.6	Surface Chemistry: Mathematical Details and Gas-Grain Models . . . . .	42
1.6.1	Rate Equations . . . . .	42

---

\*Also Departments of Astronomy and Chemistry.

1.6.2 Stochastic Approaches . . . . .	45
1.6.3 Gas-Grain Models of Cold Cores . . . . .	47
References . . . . .	50

We review the chemical processes that occur in cold (10 K) and dense ( $n \approx 10^4 \text{ cm}^{-3}$ ) interstellar cores, which are the coldest objects in larger assemblies of gas and dust known as dense interstellar clouds. We show how these processes produce the wide variety of exotic and normal molecules detected in these portions of the interstellar medium. Although much of the chemistry occurs in the gas phase, a significant portion takes place on the surfaces of the dust particles. Both types of chemistry are discussed. Some emphasis is placed on deuterium isotopic fractionation, which enhances the abundances of deuterium-containing isotopologues by very large factors compared with the low deuterium-to-hydrogen elemental abundance ratio of  $\approx 10^{-5}$ . The strengths and weaknesses of large time-dependent models of the chemistry are discussed.

## 1.1. Introduction

Baryonic matter in the universe is localised to a great extent in large assemblies of stars and interstellar matter known as galaxies. Galaxies come in a variety of shapes and sizes (e.g. spiral, elliptical, irregular, giant, dwarf); ours, the Milky Way, is a rather typical specimen of the spiral variety and has a baryonic mass of roughly  $10^{11}$  solar masses. Except for a halo around the galactic centre, the Milky Way is rather flat, with its spiral arms tracing out high densities of material. Approximately 10% of the matter lies in between the stars. In external galaxies, the amount of interstellar matter can be significantly less. Careful study of the spectra of stellar atmospheres in which the matter is mainly atomic yields the relative abundances of each element. Although all stars are not the same in this regard, average or “cosmic abundances” are well-known for our galaxy and tell us that the Milky Way consists mostly of hydrogen, with the abundance of helium roughly 10% of that of hydrogen by number. Both of these elements were produced in the Big Bang. All heavier elements, which are produced in stellar interiors, have much lower abundances. For example, the biogenic elements carbon, nitrogen, and oxygen have abundances relative to hydrogen of  $3 \times 10^{-4}$ ,  $9 \times 10^{-5}$ , and  $7 \times 10^{-4}$ , respectively. The abundance of deuterium is somewhat variable but is roughly  $1\text{--}2 \times 10^{-5}$  that of hydrogen throughout much of our galaxy. Elemental abundances need not be the same in other galaxies; for example, the abundances of elements heavier than helium, known collectively as the “metallicity” despite the fact that the most abundant elements are certainly not metals, can be much lower in nearby irregular galaxies.

The so-called interstellar medium is rather heterogeneous in density and temperature.<sup>1,2</sup> Molecules exist in the colder portions of the medium, which consists of “clouds” of varying density that can be labelled as “diffuse” or “dense” and contain matter both in the form of gas and tiny dust particles. Diffuse clouds are rather transparent to the radiation of background stars whereas dense clouds have sufficient material to be opaque to background stars in the visible and ultra-violet regions of the spectrum. The opacity is due mainly to the dust particles, and its wavelength dependence can be used to estimate their size distribution. The typical gas-phase temperature in a diffuse cloud lies between 50–100 K with densities  $n$  in the range  $10^{2-3} \text{ cm}^{-3}$ . Although a small number of diatomic and triatomic gas-phase molecules have been detected in these regions, they are of low fractional abundance except for molecular hydrogen, which can have a concentration as large as its atomic form. Since dust particles tend to be formed out of heavy refractory elements, these are reduced in abundance compared with stellar cosmic abundances. Typical “depletions” in diffuse clouds range from factors of a few for carbon and oxygen to much greater factors for refractory elements such as silicon, iron, and calcium.

Although small and relatively homogeneous dense clouds, known as globules, can occur by themselves, the larger dense clouds are quite heterogeneous in density, and depending on size are known as “assemblies” or “giant” clouds. In these large objects, the dense matter often exists as “cold cores” in a bath of more diffuse material, which can be as rarefied as in diffuse clouds or somewhat denser. These cold cores, with a size of a light year ( $9.46 \times 10^{17} \text{ cm}$ ) or less, a temperature of 10 K, and a density  $n = 10^4 \text{ cm}^{-3}$ , are presumably formed from their surroundings by gravitational collapse. Their temperature is still significantly above the black-body background temperature of the universe, 2.728 K, which shows that there are additional sources of heat. The background material surrounding the cores is typically somewhat warmer, ranging in temperature up to  $\approx 25 \text{ K}$  for the more diffuse portions. In the dense gas, there is very little atomic hydrogen; the conversion from atomic to molecular hydrogen is essentially complete. Indeed, large numbers of gas-phase molecules can be detected, mainly through their rotational emission spectra. The two-best known cold cores are labelled TMC-1 and L134N; in the former, more than 50 different gas-phase molecules have been detected. The gas-phase elemental abundances in these objects can be difficult to determine since much of the matter is no longer in atomic form. Nevertheless, models of the chemistry work best with higher depletions for selected heavy elements than observed in diffuse clouds.

Cold cores are not stable indefinitely; some disperse while others collapse further. The collapse, which leads to the formation of solar-type stars,

proceeds initially in an isothermal manner, since molecules radiate away the kinetic energy developed in the collapse. Eventually, a central dense condensation develops, which can have a temperature perhaps as low as 5 K and a density of  $10^6 \text{ cm}^{-3}$  or more. Such objects are known as “pre-stellar cores.” Once the central condensation becomes sufficiently dense to be optically thick to cooling radiation, it can no longer remain cool but starts to heat up, becoming what is known as a “protostar”, which emits in the infrared. As the protostar heats up, it warms its environment and this material becomes known as a hot corino.<sup>1</sup> Larger and warmer structures, known as hot cores, are associated with high-mass star formation. With temperatures ranging from 100–300 K depending upon the mass of the protostar, hot cores and corinos show a rich chemistry that is quite different from their colder forebears. Meanwhile, the central protostar becomes hot enough to ignite nuclear reactions and becomes a baby star. Some of the surrounding material collapses into a planar rotating disk of dense gas and dust, known as a “protoplanetary disk”. In some instances, the dust in the disk can agglomerate into larger solid objects such as planetary systems. As the star-planet system develops, it can blow off the surrounding material. Before this event occurs, the nascent stars can strongly radiate the region around them and produce so-called photon-dominated regions.

### 1.1.1. *Interstellar Molecules and Their Chemistry*

Table 1.1 lists the gas-phase molecules detected in all phases of the interstellar medium, mainly dense clouds, and in very old stars that have developed a large circumstellar shell of gas and dust similar in physical conditions to cold interstellar cores. The molecules range in size from simple diatomics to a thirteen-atom nitrile, and are overwhelmingly organic in nature.<sup>3</sup> The second most abundant molecule to  $\text{H}_2$  in dense regions is CO, which has a so-called fractional abundance with respect to  $\text{H}_2$  of  $10^{-4}$ . A large percentage of the molecules are exotic by terrestrial standards, including positive and negative molecular ions, radicals, and isomers. Molecular positive ions have fractional abundances of at most  $10^{-8}$ ; these are for the least reactive of such species. The most abundant polyatomic species have fractional abundances of  $10^{-6}$ . Moreover, most of the organic species found in cold cores are very unsaturated, such as the radical series  $\text{C}_n\text{H}$  and the cyanopolyynes series ( $\text{HC}_{2n}\text{CN}$ ), while more saturated, terrestrial-type organic species such as methanol, ethanol, methyl formate, propionitrile, etc. are associated with hot cores/corinos either because their abundance is higher in such sources or because they are only found there.<sup>1</sup>

In the cooler portions of large dense clouds, the dust particles can be studied by vibrational absorption spectroscopy using both ground-based

Table 1.1. Gas-phase interstellar and circumstellar molecules

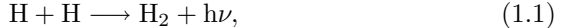
H <sub>2</sub>	PO	N <sub>2</sub> O	CH <sub>4</sub>	C <sub>4</sub> H <sub>2</sub>	H <sub>2</sub> C <sub>6</sub>
CH	SO	SO <sub>2</sub>	SiH <sub>4</sub>	H <sub>2</sub> C <sub>4</sub>	C <sub>6</sub> H <sub>2</sub>
CH <sup>+</sup>	SO <sup>+</sup>	SiCN	H <sub>2</sub> COH <sup>+</sup>	HC <sub>2</sub> CHO	C <sub>7</sub> H
NH	FeO	SiNC	CH <sub>2</sub> NH	c-C <sub>3</sub> H <sub>2</sub> O	
OH		AlNC	H <sub>2</sub> C <sub>3</sub>	HC <sub>3</sub> NH <sup>+</sup>	CH <sub>3</sub> CHCH <sub>2</sub>
SH	H <sub>3</sub> <sup>+</sup>	MgCN	c-C <sub>3</sub> H <sub>2</sub>	C <sub>5</sub> N	CH <sub>3</sub> OCH <sub>3</sub>
C <sub>2</sub>	CH <sub>2</sub>	MgNC	CH <sub>2</sub> CN	HC <sub>4</sub> N	CH <sub>3</sub> CONH <sub>2</sub>
CN	NH <sub>2</sub>		NH <sub>2</sub> CN		CH <sub>3</sub> C <sub>4</sub> H
CO	H <sub>2</sub> O	CH <sub>3</sub>	CH <sub>2</sub> CO		C <sub>8</sub> H
CO <sup>+</sup>	H <sub>2</sub> S	NH <sub>3</sub>	HCOOH	CH <sub>3</sub> CHO	C <sub>8</sub> H <sup>-</sup>
CF <sup>+</sup>	CCH	H <sub>3</sub> O <sup>+</sup>	C <sub>4</sub> H	CH <sub>3</sub> NH <sub>2</sub>	HC <sub>7</sub> N
CP	HCN	H <sub>2</sub> CO	C <sub>4</sub> H <sup>-</sup>	CH <sub>3</sub> CCH	
CS	HNC	HCCH	HC <sub>3</sub> N	C <sub>2</sub> H <sub>3</sub> OH	C <sub>2</sub> H <sub>5</sub> CHO
HF	HCO <sup>+</sup>	H <sub>2</sub> CN	HC <sub>2</sub> NC	c-CH <sub>2</sub> OCH <sub>2</sub>	CH <sub>3</sub> COCH <sub>3</sub>
NO	HOC <sup>+</sup>	HCNH <sup>+</sup>	HNCCC	C <sub>2</sub> H <sub>3</sub> CN	HOCH <sub>2</sub> CH <sub>2</sub> OH
PN	HCO	H <sub>2</sub> CS	C <sub>5</sub>	HC <sub>5</sub> N	CH <sub>3</sub> C <sub>5</sub> N
NS	HN <sub>2</sub> <sup>+</sup>	C <sub>3</sub> H	C <sub>4</sub> Si	C <sub>6</sub> H	
AlF	HCP	c-C <sub>3</sub> H		C <sub>6</sub> H <sup>-</sup>	CH <sub>3</sub> C <sub>6</sub> H
AlCl	HNO	HCCN			HC <sub>9</sub> N
NaCl	HCS <sup>+</sup>	HNCO	C <sub>2</sub> H <sub>4</sub>	C <sub>2</sub> H <sub>6</sub>	
KCl	C <sub>3</sub>	HOCO <sup>+</sup>	CH <sub>3</sub> OH	HCOOCH <sub>3</sub>	C <sub>6</sub> H <sub>6</sub>
SiC	C <sub>2</sub> O	HNCS	CH <sub>3</sub> SH	CH <sub>3</sub> COOH	
SiN	C <sub>2</sub> S	C <sub>3</sub> N	CH <sub>3</sub> CN	HOCH <sub>2</sub> CHO	HC <sub>11</sub> N
SiO	c-C <sub>2</sub> Si	C <sub>3</sub> O	CH <sub>3</sub> NC	C <sub>2</sub> H <sub>3</sub> CHO	
SiS	CO <sub>2</sub>	C <sub>3</sub> S	CH <sub>2</sub> CNH	CH <sub>3</sub> C <sub>3</sub> N	
N <sub>2</sub> ?	OCS	c-SiC <sub>3</sub>	NH <sub>2</sub> CHO	CH <sub>2</sub> CCHCN	

Notes: “c” stands for cyclic species; “?” stands for ambiguous detections; isotopologues excluded. (August 2007)

and space-borne spectrometers with either protostars or background stars as the lamp.<sup>2,4</sup> In this manner, it is found that dust particles are core-mantle objects, with cores mainly of amorphous silicates and mantles of mixed ices containing water, CO<sub>2</sub>, CO, methanol, and other species with lesser abundances. These mantles evaporate as hot cores are formed, and their molecular inventory becomes part of the gas phase, accounting in part for the chemical differences between cold and hot cores.<sup>1</sup> There is also evidence for small particles of amorphous carbon ranging down in size to large molecules known as PAH’s (polycyclic aromatic hydrocarbons), which are associated with the soot formed in combustion on Earth.<sup>2</sup>

Interstellar molecules are formed in the clouds themselves from atoms and dust particles ejected from older stars, either explosively, as in the case of supernovae, or less violently, as in the case of low-mass stars. The stellar ejecta eventually lead to the formation of interstellar clouds through the force of gravity, which also causes the formation of denser smaller structures

mediated possibly by turbulence, shock waves, and ambipolar diffusion. During the early stages of cloud formation, the diffuse material is rather inhospitable to molecular development, because the density is low and photons penetrate the regions so as to photodissociate species. Nevertheless, molecular hydrogen is formed efficiently.<sup>2</sup> Under low-density conditions, the only gas-phase process capable of producing a diatomic species from precursor atoms is radiative association, in which the diatomic complex is stabilised by the emission of a photon. This process,



is very inefficient for a variety of reasons and cannot possibly explain the large abundance of molecular hydrogen.<sup>2</sup> Alternative associative processes, which are important in the high-temperature early universe, involve ions; e.g.,



These processes are too slow to produce much  $\text{H}_2$  under cold interstellar conditions. The only viable alternative is the formation of  $\text{H}_2$  on dust particles by successive adsorption of two hydrogen atoms. In the last decade, experiments and theory have shown that the process is an efficient one on a variety of amorphous and irregular surfaces over a range of temperatures that include those of diffuse and dense interstellar clouds.<sup>1</sup> Moreover, the exothermicity of reaction can provide enough energy to desorb the newly-formed  $\text{H}_2$  from the dust particle, often in excited vibrational states.<sup>5</sup> After a significant amount of gaseous  $\text{H}_2$  is produced, it can shield itself against photodissociation since this process occurs via line radiation to specific states of an excited electronic state followed by emission to the continuum of the ground state. The discrete radiation needed is then more strongly diminished than continuum radiation.<sup>2</sup>

Once there is a sizeable amount of  $\text{H}_2$  in the gas, gas-phase reactions can occur, and lead to the production of most but not all of the species seen in diffuse clouds and dense cores. At the same time, in the cold dense regions, molecules in the gas slowly adsorb onto dust particles. Some are unreactive on surfaces, whereas others, mainly atoms and radicals, are reactive. The result is that mantles of ice grow with the most abundant species formed by chemical reaction rather than simple deposition from the gas.<sup>2,6</sup>

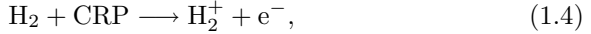
The gas-phase chemistry in cold cores is strongly constrained by the low density and the low temperature. The former condition rules out three-body processes such as ternary association, whereas the latter rules out ordinary

chemical reactions, which possess significant amounts of activation energy. After all, with a standard Arrhenius expression for the rate coefficient, an activation energy of 1 eV or more and a temperature of 10 K lead to a very small rate coefficient and, given the long intervals between collisions, high rate coefficients, near the collisional limit, are needed. The chemical processes that dominate the gas-phase chemistry are thus exothermic reactions without activation energy. These processes comprise both reactions involving ions (e.g., ion-molecule and electron recombination reactions) and those involving one or two radicals. Actually, the role of ion-molecule processes was recognized first, and it is still reasonable to state that such processes do dominate the chemistry of cold interstellar gas.<sup>7</sup> Studies of even colder gas; viz.  $\leq 1$  K, as discussed in this volume, will improve our understanding of low-temperature chemistry and allow us to make more accurate predictions of rate coefficients at low interstellar temperatures.

Ions are formed by a variety of processes, but the dominant one is ionisation by cosmic rays, which are high energy (MeV-GeV) bare nuclei travelling at velocities near the speed of light and formed in highly energetic events such as supernovae. Although the energy spectrum of cosmic rays can be measured above the terrestrial atmosphere, the low-energy tail interacts sufficiently with the solar wind that it does not reach the orbit of the Earth. Since cosmic rays reflect cosmic abundances, they are dominated by protons. As energetic protons enter interstellar clouds, they can ionise many atoms and molecules before losing their high kinetic energies. Moreover, the secondary electrons produced in the ionisation can themselves ionise other atoms and molecules. Since the flux of cosmic rays is rather low, the fractional ionisation obtained in dense sources is only on the order of  $10^{-7}$ . The actual rate of ionisation is parameterized by a first-order rate coefficient  $\zeta$  ( $\text{s}^{-1}$ ), and is typically estimated to be in the vicinity of  $1\text{--}5 \times 10^{-17} \text{ s}^{-1}$  for dense cold cores and possibly 1–2 orders of magnitude higher in diffuse clouds.<sup>2,8</sup> These values come from estimates based on the measured cosmic ray flux above the Earth and the calculated ionisation cross section or by fitting models of the type discussed below with observed abundances of molecules. The difference between diffuse and dense sources comes from the penetration depth of cosmic rays as a function of energy; only higher energy rays can penetrate through the column of material associated with dense clouds whereas lower energy cosmic rays can penetrate through the lesser columns associated with diffuse clouds. The lower penetration depth is associated with a higher cross section for ionisation. Despite the higher value of  $\zeta$  in diffuse clouds, the major source of ionisation in such sources is ultra-violet radiation from background stars, which is sufficient to ionise the gas-phase carbon totally, leading to a fractional ionisation as high as  $10^{-4}$ . In dense clouds, on the other hand, external photons do

not penetrate and the major source of ultra-violet radiation comes from cosmic rays, which excite molecular hydrogen, which in turn fluoresces. The radiation field from this indirect process is large enough that it competes with chemical reactions in the destruction of gas-phase neutral molecules.

The most important ionisation caused by cosmic ray protons (CRP) in dense clouds is that of  $\text{H}_2$ , the dominant species:



in which the major channel is single ionisation without dissociation. The parameter  $\zeta$  normally refers to the ionisation of  $\text{H}_2$  and includes ionisation by secondary electrons. Once  $\text{H}_2^+$  is formed, it immediately (within a day or so) reacts with  $\text{H}_2$  via a well-studied ion-molecule reaction to form the well-known triangular ion  $\text{H}_3^+$ :

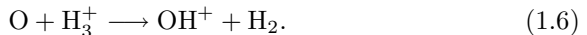


Since this ion does not react with ubiquitous  $\text{H}_2$ , it has a higher abundance than  $\text{H}_2^+$  and has been detected via vibrational transitions in both dense and diffuse clouds.<sup>9</sup> Cosmic ray ionisation of helium is also a key process; the resulting  $\text{He}^+$  ion does not react rapidly with  $\text{H}_2$ .

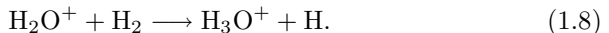
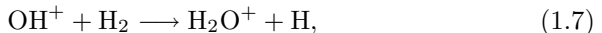
In the following section, we consider the different types of gas-phase chemical processes that occur in the cold interstellar gas, both from the point of view of their synthetic and destructive roles, and from what is known about them.<sup>2,7</sup>

## 1.2. Gas-Phase Chemical Processes

Let us start by discussing the combined roles of ion-molecule and dissociative recombination reactions in a simple synthesis, that of water and the hydroxyl radical. The first reaction in the sequence is the ion-molecule reaction between atomic oxygen and  $\text{H}_3^+$ :



The hydroxyl ion is depleted “quickly” by a hydrogen atom transfer reaction with  $\text{H}_2$ , as is the reaction product  $\text{H}_2\text{O}^+$ :



The oxonium ion,  $\text{H}_3\text{O}^+$ , does not react with  $\text{H}_2$  and instead reacts with electrons in a process known as dissociative recombination, leading to

neutral fragments such as water and the hydroxyl radical. Both of these species are then depleted by gas-phase reactions. This small subset of reactions is a paradigm of ion-molecule syntheses in cold interstellar clouds. Note that similar processes occur in diffuse clouds, but the harsh ultraviolet radiation field penetrating these clouds limits the chemistry by rapid photodissociation of species other than  $\text{H}_2$  and, to a lesser extent,  $\text{CO}$ , which are shielded by self-absorption of the distinctive radiation needed.<sup>2</sup>

### 1.2.1. *Ion-molecule and Dissociative Recombination Reactions*

Ion-molecule reactions with  $\text{H}_2$  as the neutral reactant play an important role in the chemistry of interstellar clouds. Indeed, ion-molecule reactions involving many other neutral species, non-polar and polar, are also critical. A useful compendium of ion-molecule reactions has been put together by Anicich.<sup>10</sup> Reactions with non-polar reactants such as  $\text{H}_2$  often occur with rate coefficients very close to that given by a simple capture approach known as the Langevin model, in which only the long-range ion-induced dipole potential is used and the polarisability is assumed to be a scalar so that the problem reduces to that of a central force. With the assumption that all trajectories that overcome the centrifugal barrier lead to reaction, the Langevin rate coefficient  $k_L$  is given by the expression (in cgs-esu units)<sup>11</sup>

$$k_L = 2\pi e \sqrt{\alpha/\mu}, \quad (1.9)$$

where  $\alpha$  is the polarisability,  $e$  is the electronic charge, and  $\mu$  is the reduced mass. A typical value of  $k_L$  is  $\approx 10^{-9} \text{ cm}^3 \text{ s}^{-1}$ .

For the case of polar neutral reactants, the problem is no longer one which assumes a central force.<sup>11,12</sup> The simplest treatment of such reactions — the locked-dipole approach — is a capture approach based on the assumption that the dipole stops rotating and locks onto the incoming ion in a linear configuration. The result is a large and temperature-dependent rate coefficient of the form

$$k_{LD} = [1 + (2/\pi^{1/2})x]k_L, \quad (1.10)$$

where  $k_L$  is the Langevin rate coefficient, and  $x$  (cgs-esu units) is given by the expression

$$x = \frac{\mu_D}{\sqrt{2\alpha k_B T}}. \quad (1.11)$$

Here  $\mu_D$  is the dipole moment of the neutral, and  $k_B$  is the Boltzmann constant. The result is normally too large compared with experimental

values but it is an asymptotic limit as the temperature approaches zero and the dipolar neutral loses angular momentum. In cold interstellar cores, there is also the possibility that rotation is subthermal at the low densities, so that the neutral species lie preferentially in low rotational states even at higher temperatures. For reactions involving non-linear neutral species, a more reasonable approximation, based on classical trajectory techniques, is known as the “trajectory scaling (ts) approach.” Here the rate coefficient is given by the expression

$$k_{ts} = [0.62 + 0.4767x]k_L. \quad (1.12)$$

For large  $x$ , as occurs at low temperature, the temperature dependence of both approaches is  $T^{-1/2}$ . More detailed theoretical methods exist, ranging from refined capture theories to full quantum scattering treatments.

Of course, the simple models are not always accurate, nor do they consider the role of multiple potential surfaces arising from degenerate or near-degenerate electronic states of reactants, or yield any information on the branching fractions of assorted possible exothermic products. Experimental results, performed in a variety of ways although mainly with SIFT (Selected Ion Flow Tube) and ICR (Ion Cyclotron Resonance) techniques,<sup>13,14</sup> are indeed needed by modellers. Useful compendia of measured ion-molecule rates and products exist, such as those of Anicich<sup>10</sup> and the electronic *UMIST Database for Astrochemistry*.<sup>15</sup> The many unstudied ion-molecule reactions can often be grouped into families by types of reaction, and correct products often guessed at. For example, reactions between an ion and  $H_2$  often yield products in which a hydrogen atom is transferred to the ion, as occurs in the reactions leading to  $H_3O^+$ . Eventually the sequence is terminated either because a reaction does not occur rapidly due to barriers or endothermicity, or because the saturated ion is produced. Thus, the oxonium ion does not react with  $H_2$ , but undergoes dissociative recombination with an electron. The low abundance of electrons in cold cores make such reactions much slower than ion- $H_2$  reactions, although the rate coefficients are very large, unlike the recombination of atomic ions with electrons.

Dissociative recombination reactions<sup>16</sup> have been studied via a variety of techniques, and rate coefficients with typical values  $10^{-(6-7)}(T/300)^{-0.5} \text{ cm}^3 \text{ s}^{-1}$  measured, but the assorted products proved difficult to determine for many years. The order of magnitude of the rate coefficient and the temperature dependence can be rationalised by a simple model in which reaction occurs when the reactants, which are attracted by a Coulomb long-range potential, come within a critical distance  $R_{\text{crit}}$  of one

another. This assumption leads eventually to an approximate thermal rate coefficient  $k_{\text{dr}}$  ( $\text{cm}^3 \text{s}^{-1}$ ) given by the relation<sup>17</sup>

$$k_{\text{dr}} = e^2 R_{\text{crit}} \sqrt{\frac{8\pi}{m_e k_B T}}, \quad (1.13)$$

where  $m_e$  is the rest mass of the electron. The arbitrary assumption of a 1 Å critical distance leads to an overall rate coefficient of  $1.9 \times 10^{-6} (\text{T}/300)^{-0.5}$ . Naturally, more detailed, quantum mechanical treatments have been undertaken, especially for the particularly complex case of  $\text{H}_3^+ + e$ . For most systems, two mechanisms compete with one another: a direct mechanism, in which the system crosses over into a repulsive neutral state with a potential surface that intersects that of the ion near its equilibrium geometry, and an indirect one, in which Rydberg states mediate the transfer.

Following a small number of experiments that utilised the flowing afterglow apparatus<sup>18</sup> and spectroscopic detection of neutrals, the products of a significant number of reactions have been studied with storage rings, mainly in Stockholm (CRYRING)<sup>19</sup> and in Aarhus (ASTRID).<sup>20</sup> In these latter experiments, a beam of ions is merged with electrons and, following reaction, the neutral products exit the curved beam and strike detectors, allowing a determination of their mass. For the dissociative recombination of the oxonium ion, the following product channels have been detected:  $\text{H}_2\text{O} + \text{H}$ ,  $\text{OH} + 2\text{H}$ ,  $\text{OH} + \text{H}_2$ , and  $\text{O} + \text{H} + \text{H}_2$ . The product branching fractions have been measured by the flowing afterglow method, and via two storage rings, and the experimental results vary, especially those between the two techniques. Both storage ring experiments show that  $\text{OH} + 2\text{H}$  is the dominant channel, while  $\text{H}_2\text{O} + \text{H}$  has a branching fraction of 0.18–0.25. The break-up into atomic oxygen is negligible. On the other hand, the flowing afterglow results show that there is a negligible amount of water product while the channel  $\text{O} + \text{H}_2 + \text{H}$  has a branching fraction of 0.30. Despite the disagreements, all the experiments are in agreement that three-body product channels are important.

The short reaction sequence starting with  $\text{O} + \text{H}_3^+$  illustrates how ion-molecule/dissociative recombination syntheses produce unreactive ions ( $\text{H}_3\text{O}^+$ ), normal neutral species ( $\text{H}_2\text{O}$ ), and radicals ( $\text{OH}$ ). The example is too simple to lead to the production of isomers, but the dissociative recombination involving the four-atom ion  $\text{HCNH}^+$  is thought to lead to the following three sets of products:  $\text{HCN} + \text{H}$ ,  $\text{HNC} + \text{H}$ , and  $\text{CN} + 2\text{H}$ .<sup>21</sup> Although experiments have not yet been able to distinguish between  $\text{HCN}$  and  $\text{HNC}$ , theoretical treatments indicate that they are produced in equal amount. In general, ion-molecule syntheses account at least semi-quantitatively for

much and possibly most of the exotic chemistry detected in cold interstellar cloud cores.

### 1.2.2. Neutral-Neutral Reactions

Neutral-neutral reactions are also of importance, however, as long as there is no activation energy barrier.<sup>22</sup> A useful compendium can be found in the *UMIST Database for Astrochemistry*.<sup>15</sup> For example, starting with the hydroxyl radical, neutral-neutral reactions with atoms lead to the diatomics O<sub>2</sub>, NO, and N<sub>2</sub> via well-known processes:



The reaction leading to O<sub>2</sub> has been studied down to 39 K in a CRESU (Cinétique de Réaction en Ecoulement Supersonique Uniforme) apparatus. At this temperature, the measured rate coefficient is  $3.5 \times 10^{-11} \text{ cm}^3 \text{ s}^{-1}$ . Although the CRESU result appears to be independent of temperature in the range 39–142 K,<sup>23</sup> there is some possible disagreement with other results at slightly higher temperatures. Several theoretical treatments suggest that the rate coefficient drops, possibly appreciably, at still lower temperatures.<sup>24</sup>

If one starts with the hydrocarbon radicals CH and CH<sub>2</sub> (see below), carbon monoxide can be formed by reactions with atomic oxygen:

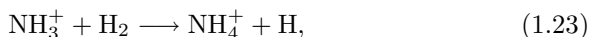
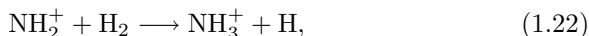
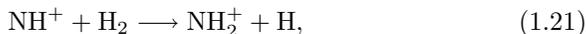
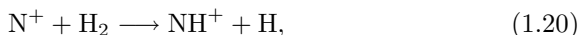


Indeed, CO is formed by many reactions, both neutral-neutral and ion-molecule, and is not easily destroyed. Not surprisingly, it is a dominant species in the cold core gas.

A particularly reactive atom in neutral-neutral reactions is atomic carbon, since, not only can it react with radicals and “semi-radicals” such as O<sub>2</sub>, it can also react with a variety of non-radicals such as unsaturated hydrocarbons. Indeed, the radicals CN and CCH have the same ability. Such reactions have been studied with the CRESU apparatus down to temperatures as low as  $\approx 10 \text{ K}$ .<sup>25,26</sup> Often the rate coefficients show a weak inverse temperature dependence below 300 K so that at low temperatures the rate coefficients can be almost as large as Langevin values. Progress has recently

been made in understanding this temperature dependence in terms of variational transition state theory<sup>27</sup> (see also Georgievskii and Klippenstein, this volume). These reactions will be discussed individually in the organic chemistry section below.

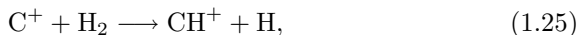
Once the diatomics CO and N<sub>2</sub> are formed, they can be protonated by reaction with H<sub>3</sub><sup>+</sup> to form the formyl ion HCO<sup>+</sup> and HN<sub>2</sub><sup>+</sup>. Neither of these species reacts with H<sub>2</sub> and so they have relatively high abundances for molecular ions (e.g., fractional abundances approaching 10<sup>-8</sup> in cold dense cores), although HN<sub>2</sub><sup>+</sup> is destroyed by reaction with CO to form the formyl ion. Other abundant ions in the gas include the atomic ions C<sup>+</sup>, H<sup>+</sup>, and He<sup>+</sup>. In addition, the existence of N<sub>2</sub> leads to ammonia via the sequence of reactions



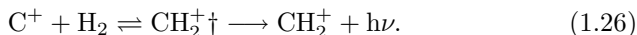
The sequence cannot begin with neutral atomic nitrogen, because its protonation reaction with H<sub>3</sub><sup>+</sup>, unlike reaction (1.6), is endothermic.

### 1.2.3. Radiative Association

If the elemental carbon is initially in the form of C<sup>+</sup>, as is detected in diffuse clouds, then the initial reaction undergone by this ion is with H<sub>2</sub> but it is *not* the ion-molecule reaction



since this process is endothermic by 0.4 eV; rather it is an unusual, low-density process known as radiative association,<sup>11</sup> in which the collision complex is stabilised by emission of a photon:



Although radiative association has been occasionally studied in the laboratory (e.g., in ion traps<sup>28</sup>), most experiments are undertaken at densities high enough that ternary association, in which collision with the background gas stabilises the complex, dominates. A variety of statistical treatments, such as the phase-space theory, have been used to study both radiative and ternary association.<sup>29</sup> These approximate theories are often quite reliable in their estimation of the rate coefficients of association reactions. In the more detailed treatments, microscopic reversibility has been applied to the formation and re-dissociation of the complex.<sup>11</sup> Enough experimental and theoretical studies have been undertaken on radiative association reactions to know that rate coefficients range downward from a collisional value to one lower than  $10^{-17} \text{ cm}^3 \text{ s}^{-1}$  and depend strongly on the lifetime of the complex and the frequency of photon emitted.<sup>11,28,29</sup> The lifetime of the complex is related directly to the density of vibrational states, a key parameter in statistical theories, which is determined by the size of the complex and its bond energy. The type of photon emitted — either between vibrational levels in the ground electronic state of the complex or between a reachable excited electronic state and the ground state — determines in part the stabilization rate. If stabilization occurs via transitions from vibrational levels of the ground electronic state above the dissociation limit to such levels below the limit, its rate can be equated with the average Einstein  $A$  coefficient for vibrational emission ( $\text{s}^{-1}$ ) in a system of coupled oscillators, which has been shown to be given approximately by the relation<sup>11</sup>

$$A = (E_{\text{vib}}/s) \sum_{i=1}^s A_{1-0}^{(i)}/h\nu_i \quad (1.27)$$

where  $E_{\text{vib}}$  is the vibrational energy with respect to the potential minimum,  $s$  is the number of oscillators,  $A_{1-0}^{(i)}$  is the Einstein emission rate for the fundamental transition of the individual mode  $i$  and the sum is over the modes  $i$  with frequencies  $\nu_i$ .

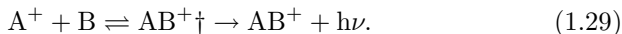
The association of  $\text{C}^+$  and  $\text{H}_2$  has a calculated rate coefficient, derived from a statistical theory, of  $4 \times 10^{-16} (T/300)^{-0.2} \text{ cm}^3 \text{ s}^{-1}$  in the range 10–300 K.<sup>30</sup> Although the rate coefficient is small, the fact that  $\text{H}_2$  is a reactant makes the process competitive. A variety of other radiative association processes are important in interstellar chemistry, perhaps the simplest being the corresponding reaction involving neutral atomic carbon:



which, however, has not been studied in great detail. Often, there is laboratory information on the ternary association but not the radiative one.

In this case, one can make a partial use of theory to convert the experimental information into an estimate for the radiative association rate coefficient.<sup>11,29</sup>

Consider a radiative association between an ion  $A^+$  and a neutral  $B$  that occurs via a complex  $AB^+\dagger$ :



If we label the rate coefficients for formation, dissociation, and radiative stabilization of the complex  $k_1$ ,  $k_{-1}$ , and  $k_r$  respectively, the steady-state approximation yields that the second-order rate coefficient  $k_{\text{ra}}$  for radiative association is

$$k_{\text{ra}} = \frac{k_1 k_r}{k_{-1} + k_r} \approx (k_1/k_{-1})k_r, \quad (1.30)$$

assuming, as is most often the case, that the dissociation rate exceeds the radiative stabilization rate. If a quasi-thermal theory is used, the ratio  $k_1/k_{-1}$  can be treated as an equilibrium constant, while if phase-space theory is used, one must compute a value of  $k_1$  for each initial state of the reactants and the overall rate coefficient involves a summation over the states of the reactants and the angular momentum of the complex. A state-specific treatment of some type is necessary to obtain the correct density dependence for association over the whole range of densities, especially at high densities, when ternary association gives way to a saturated two-body rate law. A similar steady-state analysis to that used for Eq. (1.30) for ternary association yields the third-order rate coefficient  $k_{3B}$ :

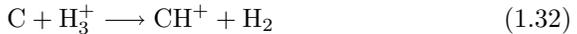
$$k_{3B} \approx (k_1/k_{-1})k_2, \quad (1.31)$$

where  $k_2$  is the rate coefficient for collisional stabilization of the complex. Conversion of  $k_{3B}$  into  $k_{\text{ra}}$  then requires knowledge only of  $k_2$  and  $k_r$ .<sup>29</sup> The collisional stabilization rate coefficient depends on the bath gas, which is often helium for ion-molecule systems. The efficiency is found to be less than unity, and it is typical to approximate this rate coefficient in the range  $\approx 10^{-9} - 10^{-10} \text{ cm}^3 \text{ s}^{-1}$  for ion-helium relaxation, with the lower limit appropriate for room temperature.<sup>29</sup> The radiative stabilization rate via vibrational photons is given by Eq. (1.27) for the average Einstein  $A$  coefficient. For a standard bond energy of 4 eV and typical fundamental intensities,  $k_r \approx 10^{2-3} \text{ s}^{-1}$ . To convert  $k_{\text{ra}}$  to a lower temperature, as is often needed, one can use the temperature dependence from the quasi-thermal approach of Bates & Herbst,<sup>29</sup> in which the rate coefficient for radiative association goes as  $T^{-r/2}$ , where  $r$  is the total number of rotational degrees of freedom of the reactants assuming that rotation can be treated classically. For light reactants, especially  $\text{H}_2$ , this approximation is poor and it

is better to ignore its two rotational degrees of freedom. As an example, suppose a reaction between  $A^+$  and  $B$  is measured to have a ternary rate coefficient at 300 K of  $10^{-27} \text{ cm}^6 \text{ s}^{-1}$ . Using  $k_2 = 10^{-10} \text{ cm}^3 \text{ s}^{-1}$  and  $k_r = 10^2 \text{ s}^{-1}$ , we obtain that  $k_{\text{ra}} = 10^{-15} \text{ cm}^3 \text{ s}^{-1}$  at room temperature, with a temperature-dependent rate coefficient of  $k_{\text{ra}} = 10^{-15} (T/300)^{-3} \text{ cm}^3 \text{ s}^{-1}$ , where it has been assumed that the reactants are non-linear species with three degrees of rotational freedom each. Of course, this approach is a crude one because the individual rate coefficients are highly averaged quantities.<sup>29</sup> An alternative approach is to use a statistical method for the exact temperature dependence, since this can be more complex if rotation cannot be treated classically, if there is atomic fine structure, and for other reasons as well.<sup>30</sup>

#### 1.2.4. Organic Chemistry

In addition to the basic radiative association between  $C^+$  and  $H_2$ , the reaction

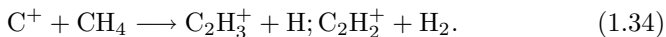


also serves to “fix” atomic carbon into a molecular form and thus start the build-up of organic molecules, or, more specifically, hydrocarbons. This proton-transfer reaction has yet to be studied in the laboratory. Once  $CH^+$  and  $CH_2^+$  are produced, H-atom transfer reactions with  $H_2$  lead to the methyl ion,  $CH_3^+$ . Like  $C^+$ , the methyl ion does not react exothermically with  $H_2$  but does undergo a radiative association to form  $CH_5^+$ , which has been studied in two different laboratories and via statistical theory.<sup>28</sup> Although the three approaches are not in perfect agreement, an estimated value for  $k_{\text{ra}}$  of  $1.3 \times 10^{-14} (T/300)^{-1.0} \text{ cm}^3 \text{ s}^{-1}$  in the range 10–300 K is used in interstellar model networks. Note that the radiative association rate coefficient is larger for the reaction involving more atoms. Interestingly, at 10 K the radiative association of  $CH_3^+$  with  $H_2$  is faster than dissociative recombination because of the low abundance of electrons. Once  $CH_5^+$  is produced, it can undergo dissociative recombination with electrons to form a variety of single-carbon hydrocarbons, although methane is a minor product. This species is formed more efficiently by the reaction



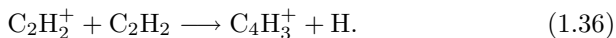
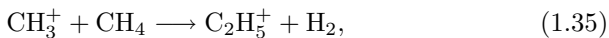
The formation of more complex hydrocarbons then proceeds via three types of processes — carbon “insertion”, condensation, and radiative association of heavy species — which can occur for both ion-molecule and neutral-neutral reactions.<sup>2,7</sup> Many of the ion-molecule reactions important in both synthesis and depletion have been tabulated in either experimental

compilations<sup>10</sup> or compilations based on interstellar networks.<sup>15</sup> In the ion-molecule realm, both  $C^+$  and neutral atomic carbon can undergo a variety of insertion reactions. Note that by the term “insertion”, we do not mean that the attacking carbon atom/ion must insert itself into a chemical bond, but also that it can add itself to a terminal atom. Many reactions involving  $C^+$  and hydrocarbons have been studied, and these often show products in which the insertion/addition of the carbon leads to a more complex but less saturated hydrocarbon. Consider, for example, the reaction between  $C^+$  and methane:



Experimental studies show that the first set of products dominates with a branching fraction of 0.73.<sup>10</sup> Reactions between neutral atomic carbon and hydrocarbon ions are thought to also lead to carbon insertion, but experiments are lacking. Without H-atom transfer or radiative association reactions with  $H_2$ , carbon-insertion reactions eventually lead to bare clusters ( $C_n$  or  $C_n^+$ ). For example, consider the case of  $C_2H_3^+$ , which undergoes no reaction with  $H_2$ . Instead, dissociative recombination occurs to form species such as  $C_2H$  and  $C_2H_2$ . Reactions with  $C^+$  then lead to ions such as  $C_3^+$  and  $C_3H^+$ . These ions react with  $H_2$  to form hydrocarbon ions only as saturated as  $C_3H_3^+$ , which is partly isomerised to a cyclic form. Dissociative recombination leads to *c*- $C_3H_2$ , *c*- $C_3H$ , as well as the linear and carbene forms  $CCCH$  and  $H_2CCC$ . As the number of carbon atoms increases past four, hydrogenation reactions seem only to saturate the ions to the extent of putting two H atoms on the carbon chain. Dissociative recombination then leads to bare clusters and to radicals of the form  $C_nH$ . Although the radicals are a salient feature of cold cores, the need to detect carbon clusters via vibrational transitions has so far precluded their detection in these sources. They have been detected in the cold envelopes of old carbon-rich stars.

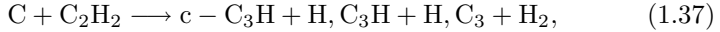
Condensation reactions also produce more complex species, and these can be somewhat more saturated. Consider, for example, the following well-studied ion-molecule examples:



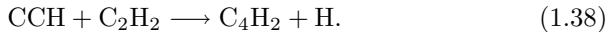
Dissociative recombination of the ethyl ion can then lead to a species as saturated as  $C_2H_4$ . Since condensation reactions are generally not as important as carbon insertion reactions, the unsaturated nature of the hydrocarbon chemistry remains a salient prediction of ion-molecule chemistry, which

appears to be in good agreement with observations of cold interstellar cores.

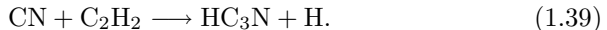
There are analogous neutral-neutral processes to the ion-molecule carbon insertion and condensation mechanisms. Reactions between unsaturated hydrocarbons and neutral atomic C often result in carbon insertion. The best-analysed reaction of this class is<sup>31,32</sup>



which has been studied via the CRESU technique, a merged-beams apparatus, and a crossed-beams apparatus. Note that both the cyclic and linear isomers of  $\text{C}_3\text{H}$  are formed. Indeed, this reaction appears to be the most important for the formation of the  $\text{C}_3\text{H}$  isomers, although the more abundant cyclic  $\text{C}_3\text{H}_2$  isomer is formed predominantly not by a neutral-neutral reaction but via the ion-molecule synthesis discussed above. For condensation reactions, a well-studied reaction is the following:<sup>25</sup>



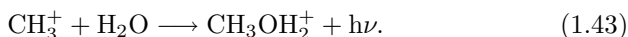
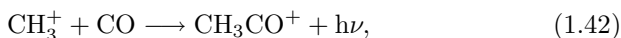
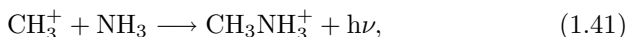
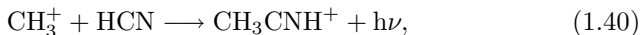
Let us now broaden our discussion to consider organic species more complex than hydrocarbons. The reaction between  $\text{C}^+$  and ammonia leads to the  $\text{HCNH}^+$  ion, which is the precursor of HCN and its isomer HNC, in addition to CN, as discussed above. The radical CN is especially reactive with unsaturated hydrocarbons at low temperatures, as shown in CRESU studies. The reaction with acetylene leads to cyanoacetylene, a well-known interstellar molecule:<sup>25</sup>



Presumably the higher members of the cyanopolyne series detected in cold cores are produced via analogous reactions between CN and  $\text{C}_4\text{H}_2$ ,  $\text{C}_6\text{H}_2$ , etc. There are competitive ion-molecule pathways, starting with reactions involving atomic nitrogen and hydrocarbon ions. Also, the two isomers of  $\text{HC}_3\text{N}$  - HNCCC and HCNCC — detected in the cold core TMC-1, are likely produced via protonation of  $\text{HC}_3\text{N}$  followed by dissociative recombination to form the unusual structures.

In addition, a number of organic species are produced from precursor ions that are the products of radiative association reactions. Although radiative association is most important when  $\text{H}_2$  is a reactant because of the overwhelming relative abundance of  $\text{H}_2$ , such processes between two heavy species are also valuable on occasion. There are some neutral-neutral systems that have been studied, but the majority of these systems are thought to be ion-molecule ones. For the most part, the systems do not possess competitive exothermic channels, although there are exceptions,

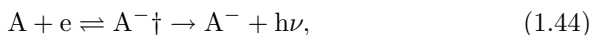
either because the collision complex can only dissociate to exothermic products with a significant barrier that does not quite choke off reaction but lengthens the lifetime of the complex, or because the association and regular channels are parallel in the sense that they take quite different pathways. The methyl ion, which is reasonably abundant because it reacts only slowly with  $\text{H}_2$ , seems to be especially fruitful as a reactant in association processes leading to more complex species. A list of such reactions involving  $\text{CH}_3^+$  follows:



The reaction involving ammonia has only been observed as a ternary process. The product ions, after dissociative recombination, should produce the neutrals  $\text{CH}_3\text{CN}$ ,  $\text{CH}_3\text{NH}_2$ ,  $\text{CH}_2\text{CO}$ , and  $\text{CH}_3\text{OH}$ , respectively. Dissociative recombination of  $\text{CH}_3\text{CNH}^+$  may also lead to the recently detected  $\text{CH}_2\text{CNH}$  (ketenimine) and the fact that  $\text{CH}_3\text{CNH}^+$  and  $\text{CH}_3\text{NCH}^+$  can reach a quasi-equilibrium means that  $\text{CH}_3\text{NC}$  can also be produced. Radiative association involving more complex hydrocarbon ions, such as  $\text{C}_2\text{H}_3^+$ , also occur with neutral reactants such as  $\text{CO}$  and  $\text{HCN}$ . Recently, however, some evidence has begun to accumulate that the radiative association processes may not be as important as previously thought. In the particular case of the formation of methanol, it appears from experimental evidence that (a) the radiative association to form protonated methanol is much slower than previously thought, and (b) the dissociative recombination reaction involving protonated methanol does not yield a significant product channel  $\text{CH}_3\text{OH} + \text{H}$ .<sup>19</sup> For the case of methyl amine, the molecule is not detected in cold cores, but in warmer ones, which argues against the involvement of radiative association, since this type of reaction gets slower with increasing temperature.

### 1.2.5. Negative Ion Formation

Many years ago, one of us<sup>33</sup> suggested that negative molecular ions could be formed in space via the process of radiative attachment. The simplest treatment of this process<sup>33,34</sup> is to assume that it proceeds via a collision complex:



where the complex is a negative ion with an energy slightly above the electron affinity of the neutral. Then, the overall rate coefficient for radiative attachment  $k_{\text{ratt}}$  is given by the same expression used above for radiative association although the individual rate coefficients for  $k_1$  and  $k_{-1}$  are not the same. If one assumes that only  $s$ -wave scattering occurs, both of these rate coefficients refer to a complex with low angular momentum equal to that of the neutral reactant. Simplification of the more general phase-space result with the additional assumption that the complex relaxes quickly to its ground electronic state leads to the simple expression

$$k_{-1} = c/\rho \quad (1.45)$$

where  $c$  is the speed of light in cgs units and  $\rho$  ( $(\text{cm}^{-1})^{-1}$ ) is the density of vibrational states of the negative ion complex in its ground electronic state at a vibrational energy equal to the electron affinity. The phase space theory result for the rate coefficient of formation of the complex is given by the expression<sup>34</sup>

$$k_1 = \hbar^2 G \sqrt{2\pi/(m_e^3 k_B T)} \approx 4.98 \times 10^{-7} G (T/300)^{-1/2}, \quad (1.46)$$

where  $G$  is the ratio of the ground-state electronic degeneracy of the anion to the product of those of the reactants. If the density of vibrational states is sufficiently large that  $k_{-1} < k_r$ , then the overall rate coefficient for radiative attachment is given by  $k_1$ .

Even more so than for the case of radiative association, very little experimental information exists for radiative attachment, and the reliability of the simple phase-space treatment has not been tested. One possible problem is that the formation of the negative ion complex may require so-called ‘‘doorway’’ states known as dipole-bound states, in a similar manner to the Rydberg mechanism for dissociative recombination of positive molecular ions.<sup>35</sup> Such states have been seen in the spectra of negative ions, although a detailed calculation employing them for radiative attachment has not been attempted.

Radiative attachment is not the only mechanism for the production of anions; their production in laboratory discharges probably occurs via dissociative attachment, in which electrons attach themselves to neutrals while a chemical bond is broken; viz.,



For the most part, however, dissociative attachment is an endothermic process because even a single chemical bond is typically greater in energy than the electron affinity of the neutral. Exceptions do exist; exothermic

dissociative attachment has been suggested to form the anion  $\text{CN}^-$  from the parent neutral  $\text{MgNC}$ , which is found in the envelope surrounding the carbon-rich star IRC+10216.<sup>34</sup>

Use of the simple phase-space approach leads to the prediction that radiative attachment is most efficient ( $k_{\text{ratt}} \approx k_1$ ) for neutral species with large electron affinities (3–4 eV) and negative ions with large densities of vibrational states, requiring species, probably radicals, with more than a few atoms in size.<sup>33,36</sup> In such situations, it was predicted that the abundance ratio of the negative ion to the neutral species in cold cores could be as high as 1% or even more, assuming that the major destruction routes are so-called associative detachment reactions with atomic hydrogen:



Given the paucity of experimental studies on the rotational spectra of negative ions, this early prediction was not tested for more than 25 years. Quite recently, a number of anions have been studied in the laboratory by the Thaddeus group,<sup>37</sup> including  $\text{CN}^-$ ,  $\text{CCH}^-$ ,  $\text{C}_4\text{H}^-$ ,  $\text{C}_6\text{H}^-$ , and  $\text{C}_8\text{H}^-$ , the neutrals of which all possess large electron affinities. Of these species, subsequent searches of interstellar and circumstellar sources have so far resulted in the detection of  $\text{C}_6\text{H}^-$  and  $\text{C}_8\text{H}^-$  in the best-studied cold core TMC-1, the detection of  $\text{C}_4\text{H}^-$ ,  $\text{C}_6\text{H}^-$ , and  $\text{C}_8\text{H}^-$  in the cold, carbon-rich circumstellar envelope IRC+10216, and the detection of  $\text{C}_6\text{H}^-$  in the protostellar source L1527. Moreover, the detected abundance of  $\text{C}_4\text{H}^-$  relative to  $\text{C}_4\text{H}$  is well below 1% in IRC+10216, and the upper limit to this ratio in TMC-1 is even smaller. In qualitative agreement,<sup>36,38</sup> use of the phase-space theory (and suitable destruction routes for anions) predicts that the  $\text{C}_4\text{H}^-/\text{C}_4\text{H}$  abundance ratio will be considerably lower than that for the larger anions of this class, for which radiative attachment is predicted to occur at the collisional limit. However, the predicted ratio for  $\text{C}_4\text{H}^-/\text{C}_4\text{H}$  is still significantly higher than the observed value in IRC+10216 and the upper limit in TMC-1, so that there is astronomical evidence, at least, that the radiative attachment of electrons to  $\text{C}_4\text{H}$  is slower than predicted. Because the dipole moment of this species is also much lower than those of the neutrals  $\text{C}_6\text{H}$  and  $\text{C}_8\text{H}$ , the argument that dipole-bound states play a role in radiative attachment gains some force, since these states only appear for dipoles larger than  $\approx 2$  Debye. Of course, astronomical evidence need not be definitive, because predicted abundances rely on uncertain knowledge of physical conditions as well as possible additional formation and destructive processes for anions such as exothermic dissociative attachment channels and photo-detachment.

### 1.3. Surface Chemistry on Cold Dust Grains: Basic Considerations

Although the major interstellar reaction that occurs on the surfaces of dust particles is the formation of molecular hydrogen, more complex molecules are also thought to be formed in this manner.

#### 1.3.1. *Low-Temperature Surface Chemistry*

In both diffuse and dense interstellar clouds, the dust grains tend to be rather cold, with temperatures in equilibrium with the gas in cold dense cores and temperatures at or below  $\approx 25$  K in the warmer diffuse medium. Gas-phase species accreting onto dust particles can bind either by weak long-range (van der Waals) forces or by strong chemical forces; the former is known as physisorption and the latter as chemisorption. Since chemisorption most often occurs with an activation energy barrier, low temperature accretion is dominated by physisorption, with binding (desorption) energies  $E_D$  ranging from  $\approx 0.03$ – $0.5$  eV. These desorption energies can be measured by classical techniques or by more modern methods such as temperature-programmed desorption (TPD).<sup>39</sup> Once on the grain and thermalised to the grain temperature, the weakly-bound species can diffuse to other sites on the grain via a random-walk. The potential for such motion depends on the adsorbate, the surface material, and its morphology. For a totally regular surface, one can imagine a potential with regularly spaced wells and barriers; the former are often referred to as binding sites. The barrier heights, which we label  $E_b$ , are normally smaller than the desorption energies, but are more difficult to measure. From limited measurements augmented by quantum chemistry,  $E_b$  is found to range in size from values close to  $E_D$  to values near zero for special surfaces such as graphite. For irregular surfaces, with assorted imperfections, the potential for diffusion is certainly irregular as well, and its local character depends on the nature of the imperfection.

There are three well-discussed mechanisms for surface reactions, and they can pertain to both chemisorption and physisorption depending on the temperature range.<sup>39</sup> The best studied mechanism, which involves the diffusion of adsorbates followed by their reaction when in close proximity, is known as the Langmuir-Hinshelwood mechanism. At low temperature, this mechanism proceeds best in the absence of chemical activation energy, but can occur competitively even in the presence of small activation energy barriers because of a competition between reaction and diffusion, which also has barriers. In the absence of low-temperature tunnelling of adsorbates between binding sites, the Langmuir-Hinshelwood mechanism for a given

type of binding operates between a lower temperature limit, under which the adsorbates cannot diffuse rapidly to find reaction partners, to a higher temperature limit, where desorption is more rapid than diffusion to find the partners. Even if the surface species cannot move, there are two other mechanisms that can become operative. The first is known as the Eley-Rideal mechanism; here a gas-phase species strikes an adsorbate and the two react. Very similar is the so-called “hot atom” mechanism, in which a hot gas-phase species sticks to the surface but fails to thermalise instantly and can hop around the surface and react before thermalising.

### 1.3.2. $H_2$ Formation

Since a significant amount of molecular hydrogen is formed in diffuse clouds, where the dust particles are thought to be mainly bare, experiments and theories directed at  $H_2$  formation in such clouds either use some form of silicate or carbon, the two materials associated with bare grains. The first low-temperature experiments on  $H_2$  formation with suitable grain analogs were performed by Vidali and co-workers with a TPD apparatus, initially on olivine and amorphous carbon.<sup>40</sup> They found that the process occurs via a Langmuir-Hinshelwood mechanism, but only over a very narrow temperature range which, especially for the case of olivine, is much lower than typical surface temperatures in diffuse clouds. From this experiment, they were able to determine the desorption energies for H and  $H_2$ , the barrier to diffusion for H, and the fraction of nascent  $H_2$  molecules immediately ejected into the gas-phase. Determination of these parameters comes from a kinetic model of the reaction, in which random walk is modelled by a simple treatment involving rate equations (see Sec. 1.6). The initial interpretation that diffusion occurs classically, by thermal hopping, rather than by tunnelling, has been challenged. More recently, Vidali *et al.*<sup>41</sup> found that using a “rough” (highly irregular) silicate surface expands the range of temperatures over which  $H_2$  formation occurs efficiently to include diffuse cloud surface temperatures, in agreement with an earlier stochastic theory.<sup>42</sup>

Other studies, on porous amorphous solid water, relevant to dense interstellar clouds where the grains have icy mantles, found a more complex process, in which  $H_2$  can be formed at very low temperatures by a rapid process possibly involving tunnelling between pores, but that the desorption of  $H_2$  into the gas occurs gradually depending on the binding site.<sup>43</sup> The formation of  $H_2$  on graphite has been studied at higher temperatures, such as might pertain to photon-dominated regions. The mechanism appears to be a complex one based on chemisorption, in which the two H atoms first form long-range clusters before combining. Another experiment, undertaken at University College London by Price and co-workers, has as its major

goal determination of the vibrational-rotational state distribution of ejected  $\text{H}_2$  molecules. Current results show considerable vibrational excitation.<sup>5</sup> In the interstellar medium, such excitation might still be detectable for many years after the formation of the hydrogen molecule. A variety of theoretical treatments have been applied to the *dynamics* of  $\text{H}_2$  formation on surfaces. Clary and co-workers, in particular, have studied both the Eley-Rideal and Langmuir-Hinshelwood mechanisms on a form of graphite (HOPG) using quantum mechanical methods.<sup>44</sup>

### 1.3.3. *Reactions in Ice Mantles*

Although a large number of surface reactions have been put into gas-grain chemical models of cold interstellar cloud cores, the dominant ones for long periods of time involve atomic hydrogen, which still has an appreciable gas-phase abundance and is uniquely reactive on surfaces because of its diffusive capability at low temperatures. In addition to combining with themselves to form  $\text{H}_2$ , H atoms can react with slower-moving heavy atoms and radicals without activation energy to saturate these species. The result is a very different chemistry from that occurring in the cold gas, where unsaturated species are the norm. Some of these reactions have been studied in the laboratory, although without as much detail as applied to the study of  $\text{H}_2$  formation. Perhaps the most important sequence of reactions involves the conversion of atomic oxygen first to the hydroxyl radical and then to water. Model calculations indicate that this synthesis of water leads to far more of the water ice detected in cold cores than does simple accretion of gas-phase water, which has a rather low abundance. Another hydrogenation sequence starts with CO, which is made copiously in the gas, and leads through the radical HCO to formaldehyde, and subsequently, through the radicals  $\text{CH}_2\text{OH}$  and  $\text{CH}_3\text{O}$ , to methanol.<sup>45</sup> Two of these reactions have small chemical activation energies, but, as will be discussed below, this need not prevent their occurrence. The sequence of reactions is an important one, since there is no known gas-phase synthesis of methanol efficient enough to explain its abundance in cold cores, which means that it must be accounted for by some sort of non-thermal desorption of methanol ice.

In addition to the formation of normal isotopologues, deuterated species can also be formed, as will be discussed later. This result can happen in two ways. First, in addition to association reactions with atomic hydrogen, there are association reactions with atomic deuterium. For example, the isotopologue  $\text{CH}_2\text{DOH}$  can be formed by the following sequence of reactions:



This type of mechanism is a general one and may well occur in regions with high abundances of atomic deuterium such as the centres of pre-stellar cores, discussed in Sec. 1.5. Secondly and more specifically, atomic deuterium can react with methanol to form  $\text{CH}_2\text{DOH}$  although the exact mechanism by which this happens is not known definitively.<sup>46</sup> Surface deuteration followed by desorption may well be an important source of gas-phase fractionation, as discussed in Sec. 1.5 following a detailed discussion of gas-phase fractionation.

## 1.4. Models with Gas-Phase Chemistry

We begin this section by discussing time scales appropriate for the physical and chemical evolution of cold cores, also known as dark interstellar clouds, before discussing various models for describing the gas-phase chemistry and the uncertainty associated with such models. It should be mentioned that kinetic treatments of the chemistry are needed because the time scales to reach chemical equilibrium are far longer than the lifetimes of the clouds, and because the chemistry is powered by an external energy source.

### 1.4.1. Time Scales

The time scale for chemical evolution for a particular species can be determined crudely by consideration of the inverse of its destruction rate.<sup>2</sup> In the unshielded interstellar medium, neutral species are destroyed by the interstellar ultraviolet radiation field with photo-rates which are typically  $\sim 10^{-10} - 10^{-11} \text{ s}^{-1}$  per event, leading to time-scales of  $\sim 300 - 3000 \text{ yr}$ . Inside cold, dark cores, the presence of dust grains causes effective absorption of the UV photons with the result that time-scales are determined by binary reactions and can be written as  $[kn(X)]^{-1} \text{ s}$ , where  $k$  is an appropriate rate coefficient ( $\text{cm}^3 \text{ s}^{-1}$ ) and  $n(X)$  is the number density ( $\text{cm}^{-3}$ ) of species X. For radicals, X corresponds to reactive atoms such as C and O with  $n(X) \sim 10^{-6}n$ , where  $n$  is the total number density of the cloud, and  $k \sim 10^{-10} - 10^{-11} \text{ cm}^3 \text{ s}^{-1}$  at low temperatures. Hence the time scale is  $\sim 3 \times 10^4 \text{ yr}$  for  $n \sim 10^4 \text{ cm}^{-3}$ . On the other hand, the time scale for destruction of stable neutral molecules such as CO or  $\text{H}_2\text{O}$  can be much longer. Such species are destroyed primarily through binary reactions with abundant cations,  $\text{X}^+$ . The rate coefficients can be taken crudely to be the Langevin value,  $\sim 10^{-9} \text{ cm}^3 \text{ s}^{-1}$  with  $n(\text{X}^+) \sim 10^{-8}n$ , leading to a time scale of  $\sim 3 \times 10^5 \text{ yr}$ . These chemical time-scales should be compared with two other important time scales in cold clouds. The first is the time scale taken for accretion, or freezing out, of the gas onto the cold dust grains

which populate these cores. For gas-phase species X, this is given by:

$$t_{acc} = (S_X \pi a^2 v_X n_d)^{-1} \quad (1.51)$$

where  $S_X$  is the fraction of collisions of X with grains which actually lead to accretion and is close to unity for dust grains at 10 K,  $\pi a^2$  is the cross section  $\sigma$  of a dust grain assuming spherical, neutral particles of radius  $a$ ,  $n_d$  is the number density of dust grains per unit volume, and  $v_X$  is the mean thermal velocity of X. A more detailed form of this equation can be written to take into account the fact that grains are charged and have a size and shape distribution, which can be determined from studies of interstellar extinction. Using typical parameters for cold clouds leads to a time scale for accretion of  $t_{acc} \sim 3 \times 10^9/n$  yr, where  $n$ , the *gas* density, is measured per  $\text{cm}^3$ . To derive this formula, we have used  $a = 0.1\mu$  and converted the grain density to the gas density by the standard dust-to-gas abundance ratio of  $\approx 1 \times 10^{-12}$ .

The second important time scale is that associated with the dynamics of the cloud itself. If the core is massive enough to be dominated by its self-gravity, then the free-fall time scale, which is the time taken for gravitational collapse to high density —  $t_{ff} \sim 4 \times 10^7/n^{1/2}$  yr — is appropriate. Even if the cores are not massive enough for self-gravity to dominate, the small physical sizes of cold cores implies that the sound-crossing time,  $t_{sc} \sim L/c_s$ , a measure of the time needed to establish pressure equilibrium, where  $L$  is the size, typically  $3 \times 10^{17}$  cm, and  $c_s$  is the sound speed, is  $\sim 10^5$  yr. For  $n = 10^4 \text{ cm}^{-3}$ , one sees that the chemical, accretion and dynamical time scales are all comparable, indicating that the adoption of steady state kinetics is likely to be a poor approximation and that time-dependent solution of the chemical (and physical) evolution of the gas must be undertaken.

#### 1.4.2. *Homogeneous Sources*

Although there have been a number of models which incorporate both dynamics and chemistry, we begin by concentrating on “pseudo-time-dependent” models; that is, those in which chemical evolution occurs under fixed physical conditions. Models in which physical conditions are fixed by a single set of parameters are known as “one-point-models” and are most readily applied to clouds which have a homogeneous structure. Although they have limited applicability to real interstellar cloud cores, they have the advantage of allowing one to investigate easily the importance of particular reactions and rate coefficients and to incorporate the effects of accretion on the chemistry. A major weakness of this approach is that, in reality, the physical conditions change as the chemistry takes place, with a more appropriate starting point at much lower densities and diffuse cloud abundances.

The advent of fast computers means that it is now feasible to integrate several hundred ordinary differential equations (ODEs) describing a gas-phase chemistry of up to 10,000 reactions in cold cores. As long as the physical conditions do not alter, the system of ODEs is first-order, although non-linear, and can be integrated using standard packages. The general form of the ODE to be solved is:

$$\begin{aligned} \frac{dn(X_i)}{dt} = & \Sigma_l \Sigma_m k_{lm} n(X_l) n(X_m) - n(X_i) \Sigma_j k_{ij} n(X_j) + \Sigma_p k_{ip} n(X_p) \\ & - n(X_i) \Sigma_q k_{iq} + k_i^{des} n(X_i^d) - k_i^{acc} n(X_i) \end{aligned} \quad (1.52)$$

where the first two terms on the right-hand side represent the binary reactions which form and destroy  $X_i$ , the following two terms represent the first-order reactions which form and destroy  $X_i$ , and the final two terms represent the desorption of  $X_i$  from the grain, where it is labelled  $X_i^d$ , and accretion onto the dust. Further terms need to be added if  $X_i$  is injected to the gas from other processes at the grain surface, e.g. dissociative recombination following collisions between gas-phase cations and negatively-charged grains. Grains in cold cores are mainly negatively charged because of the greater thermal speeds of electrons as compared with heavy positive ions.

A similar set of rate equations can be written for the granular species  $X_i^d$  and can include chemical reactions, perhaps driven by interaction with UV photons or cosmic ray particles, which alter the composition of the grain mantle. Although it is relatively easy to extend the set of ODEs to include surface species and reactions, it is not clear that such an approach is valid; small number statistics means that the notion of “averages” inherent in the rate equation approach is questionable. This issue and alternative approaches to describe surface chemistry are discussed more fully in Sec. 1.6.

The set of initial conditions which must be supplied in order to integrate the system of ODEs includes the rate coefficients together with the parameters that describe the physical conditions in the cold core — number density, elemental abundances, temperature, UV radiation field, cosmic-ray ionisation rate, and grain properties: size, number density, and opacity. Of these parameters, elemental abundances are the most uncertain due to the unknown fraction of heavy elements — carbon, nitrogen, oxygen, silicon, magnesium, etc. — which are incorporated into the refractory cores or ice mantles of the dust grains. It is common if simplistic to start with atomic gas except for hydrogen, which is at least partially molecular.

A number of groups now make available sets of gas-phase rate coefficients for use in interstellar chemistry. The *UMIST Database for Astrochemistry* (the most recent version of which is also known as RATE06)<sup>15</sup> contains information on some 4500 reactions of which some 35% have been

measured experimentally, some at temperatures down to 20 K, and has been updated and released anew every 5 years or so. The UDfA database is aimed at describing both hot and cold chemistries and software is available to select the appropriate rate coefficients for particular uses. The Ohio State University group<sup>22</sup> has an alternative database of approximately the same number of reactants and reactions, but focused more on low temperature chemistry. New versions are released on irregular time scales and designated by month and year (the current relevant version of the OSU program is `osu_03_2008`). This group also releases particular data sets which have been used in published calculations, as does the Durham/Paris group.<sup>47</sup> The UDfA database assigns an uncertainty and a temperature range of applicability to each rate coefficient; these uncertainties are also available in the recent `osu` networks. The uncertainties can be translated into predicted uncertainties for model abundances and used in sensitivity calculations. The method discussed by Wakelam *et al.*<sup>48</sup> has been used recently for cold cores, and consists of running the chemical model thousands of times with individual rate coefficients picked randomly from Gaussian distributions determined by their uncertainties. The calculated abundances also show Gaussian distributions in most instances, and these can be compared with observational results. Occasionally, the abundance distributions bifurcate into two peaks, a phenomenon known as bistability; this arises because of the non-linear nature of the coupled ODEs.

Figure 1.1, calculated with the RATE06 network,<sup>15</sup> shows the typical time evolution of the carbon chemistry for a purely gas-phase model of a cold core ( $T = 10\text{ K}$ ,  $n = 10^4\text{ cm}^{-3}$ ) in which carbon is initially ionised, hydrogen is in molecular form and the elemental abundance of oxygen is greater than that of carbon (“oxygen-rich abundances”). As one can see,  $\text{C}^+$  is transformed first to neutral carbon atoms. As discussed in Sec. 1.2,  $\text{C}^+$  and C are processed into hydrocarbons before the excess of oxygen locks up “all” of the available carbon into the strongly bound CO molecule and hydrocarbon abundances decrease to their steady-state values. A comparison between such models and observations of cold cores such as TMC-1 and L134N shows that best agreement occurs at so-called early time,  $\sim 10^5\text{ yr}$ , and is strengthened by appropriate choice of the elemental abundances. A variety of criteria have been developed to quantify the degree of agreement, the simplest being the fraction of detected molecules for which observation and calculation lead to abundances within an order of magnitude of one another. The more recent approach of Wakelam *et al.*<sup>48</sup> has also been utilised. In calculations done with the `osu` network, the abundances of approximately 80% of the 40 or so molecules seen in L134N can be reproduced to within an order-of-magnitude at early-time; the agreement for the 60 or so molecules in TMC-1 is worse unless carbon-rich abundances are utilised.<sup>48</sup> The reason for this difference is that TMC-1 is uniquely

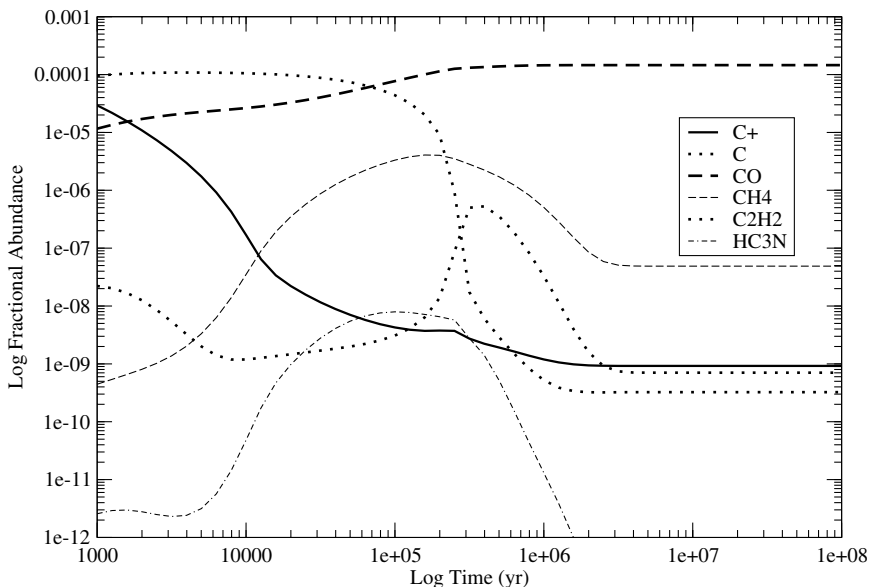


Fig. 1.1. Time evolution of gas-phase carbon chemistry at  $T = 10$  K and  $n = 10^4$  cm $^{-3}$ .

rich in organic species, and these cannot be grown very efficiently under oxygen-rich conditions. Recent work using the RATE06 network with the addition of negative ions shows that the abundance of  $C_6H^-$  in TMC-1 is well accounted for.<sup>36</sup>

As mentioned previously, steady-state abundances, which take in excess of  $10^6$  yr to be reached, are not appropriate since material will freeze out onto the dust grains, a process not included in Fig. 1.1. If one includes accretion at the standard rate, the results in Fig. 1.2 pertain. One sees that, with the exception of hydrogen and helium and their associated ions, all species are removed from the gas phase in a few million years. Since this time-scale is inversely proportional to density, then higher density cores should be unobservable via transitions in gas-phase CO. In fact, although such higher density cores exist, there is no observational evidence for *completely* depleted cores indicating that either there are mechanisms which return material, albeit inefficiently, to the gas phase or the surface area of dust grains is reduced in dense, cold cores perhaps through grain coagulation processes. Observational evidence in support of this latter conjecture is difficult to obtain using current techniques. A variety of desorption processes, discussed below, have been included in models.

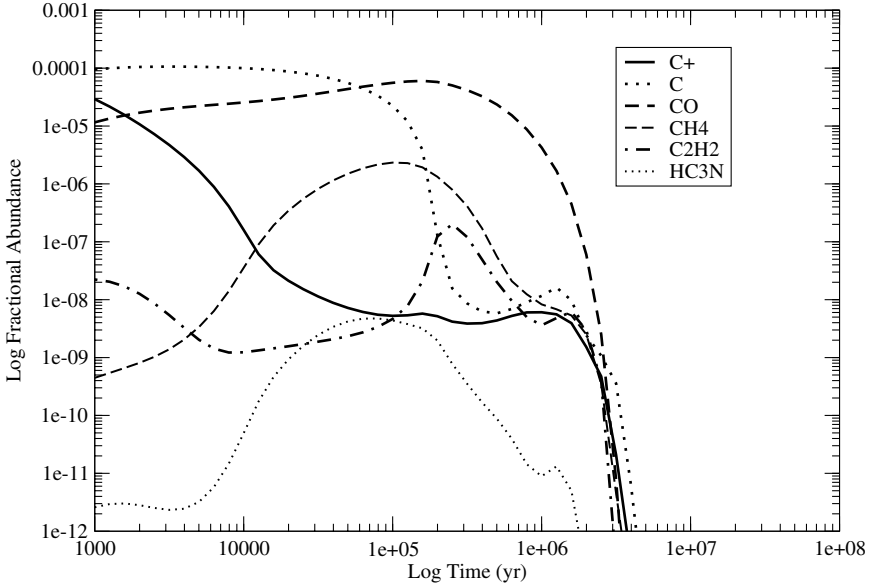


Fig. 1.2. Time evolution of gas-phase carbon chemistry but with accretion at  $T = 10$  K and  $n = 10^4 \text{ cm}^{-3}$ .

*Thermal evaporation* of a grain surface species  $X^d$  occurs with a rate coefficient<sup>2</sup>

$$k_{\text{te}} = \nu_0 e^{-E_{\text{D}}/k_{\text{B}}T_d} \quad (1.53)$$

where  $\nu_0$  is a frequency, which can be estimated as  $(2n_s E_{\text{D}}/\pi^2 m)^{1/2}$ .<sup>49</sup> Here  $n_s$  is the number of sites per unit surface area,  $m$  is the mass of the species  $X^d$ ,  $E_{\text{D}}$  is its binding (desorption) energy to the grain, and  $T_d$  is the grain temperature, which is  $\sim 10$  K in cold cores. Note that astronomers often refer to energies with units of temperature so that the Boltzmann constant  $k_{\text{B}}$  is often set to unity. Typically the frequency is about  $10^{12} \text{ s}^{-1}$  for physisorbed species. The rate of evaporation is very sensitive to the grain temperature. For example, water on water ice has a binding energy  $E_{\text{D}}/k_{\text{B}} \sim 5770$  K and a temperature rise of 10 K from  $T_d = 95$  K increases the evaporation rate by a factor of 300. For species which are weakly bound, such as CO and  $\text{N}_2$ , an even smaller temperature rise from 30 K gives the same effect. Although grain temperatures can be derived in interstellar clouds from observations of submillimeter continuum emission from dust, it is difficult to argue that the grain temperature is known to better than 10% accuracy given the uncertainties associated with their size, shape, chemical composition and emissivity, adding further uncertainty to gas-grain models. In fact, recent

experiments have shown that the situation is more complex. Astronomical infrared observations of the CO fundamental absorption band have shown that CO is trapped both within the polar, H<sub>2</sub>O-rich, component of interstellar ices as well as in the non-polar, CO- and CO<sub>2</sub>-rich, component.<sup>2</sup> Laboratory TPD experiments have shown that CO can be trapped at a variety of sites within a porous H<sub>2</sub>O ice structure and that up to four binding energies may be appropriate for this and other species.<sup>50</sup> In any case, since binding energies are typically greater than 1000  $k_B$ , the time scale for thermal evaporation from a grain at 10 K is longer than the age of the Universe. For thermal evaporation to occur within 10<sup>5</sup> yr at 10 K, one requires a binding energy less than about 550 K, not satisfied for species other than hydrogen and helium. Thus thermal evaporation is unlikely to play any significant role in returning material to the gas in cold cores.

*Cosmic ray-induced heating* refers to the passage of a high energy cosmic ray through a grain that heats material along its path of interaction and allows evaporation to occur. This process has a slow rate as the cosmic-ray ionisation rate is small and such events relatively rare.<sup>51</sup>

Absorption of external UV photons by ices can lead to *direct photodesorption* particularly at the cloud surface where the flux of UV photons is high.<sup>2</sup> If clouds are homogeneous, then the process is not competitive elsewhere due to efficient extinction of the UV field by the dust particles. The photons can penetrate the cloud more efficiently if either the surface area of the dust is much smaller than anticipated due to coagulation or the cloud is very clumpy on small scales allowing UV photons access to much greater depths from the surface. Typically, models of cold cores have ignored this desorption mechanism due to the lack of photons and the small yield of desorbed molecules per photon absorbed. Recently, it has been shown that the yield of CO desorption from CO ice is about two orders of magnitude more efficient than previously thought, indicating that it may be the dominant process at least in the outer regions of cold clouds.<sup>52</sup>

As discussed in Sec. 1.1, cosmic-ray ionisation of H<sub>2</sub> produces secondary electrons which excite H<sub>2</sub> and cause it to fluoresce in the Lyman and Werner bands. Since cosmic rays penetrate cold cores easily, these UV photons are generated internally throughout the cloud and are not subject to the levels of extinction suffered by externally-generated photons.<sup>53</sup> In principle these photons can both dissociate gas-phase molecules and photodesorb mantle material; the latter process is known as *cosmic ray-induced photodesorption*.

*Chemical reactions* can also lead to non-thermal desorption.<sup>2,5,6</sup> The formation of the H<sub>2</sub> molecule from the recombination of two H atoms on the surface of an interstellar grain releases 4.5 eV of excess energy. Much of this goes into excitation of the H<sub>2</sub> molecule but a certain fraction is deposited into the grain and may be sufficiently localised to desorb

nearby molecules. More generally, the exothermicity of any surface chemical reaction can be used to eject the products from the surface in analogy with unimolecular chemical reactions. This process will be discussed in more detail in Section 1.6.3 in the context of surface chemistry. Exothermicity-based desorption can follow photodissociation of molecules on surfaces, since the resulting fragments can recombine exothermically.

Laboratory experiments on irradiated ices result in the production of radicals which, at low temperatures, are effectively immobile in the ice. As the temperature of the ice increases, the radicals become mobile and reactions between them release energy which can be used to generate a runaway process resulting in a catastrophic desorption event or *explosion* at a temperature of about 27 K according to the experiments.<sup>2</sup> Such a temperature is too high to be achievable easily in a cold core but may occur through the absorption of a single UV photon if the grain has a very small size.

The influence of some of these desorption processes on cold core abundances has been investigated by Willacy & Williams,<sup>54</sup> Shalabeia & Greenberg,<sup>55</sup> and Willacy & Millar.<sup>56</sup> The latter also included deuterium fractionation, a process known to be efficient at low temperatures and which provides additional observational constraints. Willacy & Millar compared predictions with observations of some 25 species in the cold core TMC-1 and with the D/H abundance ratios of a further 8 species, finding best agreement (to within a factor of 5) in 19 abundances and 5 ratios for the case of H<sub>2</sub> driven desorption. The global effect of these desorption processes is to cause a quasi-steady state to develop at times in excess of a million years due to the balance between accretion and desorption. Such a quasi-steady state can also occur in models with surface chemistry, as discussed in Section 1.6.3.

Despite this apparent success, there is as yet no consensus on which, if any, of the above processes should be included in models of cold cores. Most rely on ad-hoc assumptions about efficiency, and few have been studied in the laboratory under realistic physical conditions.

### 1.4.3. *Non-Homogeneous Sources*

It is difficult to extract three-dimensional information on the physical properties of cold cores from astronomical observations. Molecular line emission traces minor components of the mass — molecular hydrogen being homopolar and therefore not possessing allowed dipole transitions — but it does have the advantage of allowing dynamical information (eg. infall, outflow, rotation) to be derived. As mentioned in the previous sub-section, there may also be other selection effects at work, for example, high-density

regions may have very weak line emission because of accretion. In such cases, thermal emission from dust grains is a better tracer of the mass distribution in the cloud. Submillimeter observations of dust emission are now used routinely to derive density and temperature profiles of the dust under some simplifying assumptions about geometry and emissivity of the particles. Such observations show that cold cores, particularly those involved in low mass star formation, have power-law density distributions, sometimes with a flatter profile or constant density in the central regions. Quiescent cores; that is, those which show thermal line widths, have density profiles well fit by those of the Bonnor-Ebert (BE) sphere, appropriate for an isothermal object in pressure equilibrium with an external medium. The BE sphere has a uniform density inner region surrounded by an envelope with density  $\rho \propto r^{-2}$ , approximately.<sup>57</sup>

For quiescent cores, the simplest approach is to model the cloud as a series of concentric shells treating each shell as a one-point model with fixed physical conditions. Such models have been constructed by Roberts *et al.*<sup>58</sup> in their study of deuterium fractionation in the pre-stellar cores L1544 and  $\rho$  Oph D. These cores were modelled by at most 6 shells and much better agreement with observation was obtained than through using a single one-point model. The non-homogeneous models, which have high densities in their central regions, show that molecular distributions such as CO will have central “holes” in their distributions due to accretion and that the size of such holes increases with increasing time. Such central holes, although detected in some species such as CS, are not detected in all molecules for reasons which are not yet clear. Thus, while CO is depleted,  $\text{N}_2\text{H}^+$  is not, despite the fact that laboratory studies show that CO and  $\text{N}_2$  have very similar binding energies on ices.<sup>59</sup> Indeed Tafalla *et al.*<sup>60</sup> find that  $\text{N}_2\text{H}^+$  has a constant abundance and that  $\text{NH}_3$  actually increases toward the core centre. Clearly, a model in which accretion and evaporation are described by essentially one parameter for each species, namely the binding energy, will be limited in its success in explaining the diversity of results seen in cold cores.

Since stars do actually form in such regions it may also be appropriate to include dynamics, particularly that of infall which is detected at velocities of about  $0.1\text{--}0.2 \text{ km s}^{-1}$  in several well-studied objects. Lee, Bergin & Evans<sup>61</sup> combined chemistry, dynamics, and a calculation of molecular excitation to follow the evolution of molecular rotational line profiles. Their model used a sequence of BE spheres and the so-called “inside-out” collapse to follow the chemistry of a parcel of gas as it falls towards the centre of the source. The results show complex, time-dependent effects in which molecular abundances are affected by the competition between accretion and evaporation. The species which has the most effect on the chemistry

is CO, not surprisingly since it is the most abundant interstellar molecule after H<sub>2</sub>. When CO is abundant in the gas phase, reaction with He<sup>+</sup> produces C<sup>+</sup> and O which proceed to form C-bearing and O-bearing molecules. When CO is frozen onto dust grains then the abundances of these other molecules decrease appreciably.

Aikawa *et al.*<sup>62</sup> have included deuterium chemistry in a BE sphere model to which infall has been added. Infall is determined by the ratio of gravitational and pressure forces with the low infall velocities observed in starless cores reproduced when the ratio is slightly greater than 1. The model contains accretion, desorption and surface chemistry using the diffusive rate approach (see Sec. 1.6). For a ratio of 1.1, a sphere with an initial central density of  $2 \times 10^4 \text{ cm}^{-3}$  takes  $1.17 \times 10^6 \text{ yr}$  to reach a central density of  $3 \times 10^7 \text{ cm}^{-3}$ , with a flat density distribution within 4000 astronomical units ( $1 \text{ AU} = 1.5 \times 10^{13} \text{ cm}$ ) and a density profile scaling as  $r^{-2.3}$  outside this. The infall is rather slow and, since both the central and outer boundary of the cloud are assumed to have zero velocity, the infall velocity has a maximum value at a radius which moves inwards as the collapse proceeds. This model reproduces the observational result that molecules such as CS and CO are depleted significantly inside 5000 AU by accretion onto grains. It is perhaps worth noting at this point that such depletions are difficult to observe, particularly for CO since the size of the depleted region is small compared to typical telescope beam sizes, and emission from CO is dominated by the outer regions of the cloud where it is undepleted rather than by the central high-density core.

These dynamical models of cold cores are typically much more complex than static models and it is worth asking whether such models actually help better constrain the physics and chemistry of star formation. Lee *et al.*<sup>63</sup> have tried to answer this question by comparing dynamical models of collapse with static models having empirical abundance distributions. Such models also seek to reproduce line profiles but do so by modifying abundance distributions, for example by adopting large steps in abundance to represent material either accreted onto or removed from grain surfaces. Such models do not contain any chemistry and are mostly used by observers to make a fit to observations so that evidence that such distributions arise naturally in dynamic models would be powerful support for the observationally-derived picture. Lee *et al.* also considered non-homogeneous, non-dynamic models and showed that differences occur between these and dynamic models even when one adopts the underlying density and temperature for the core from dust continuum observations. As mentioned above, these non-dynamic models allow large central holes to occur in the molecular distributions as material freezes rapidly on to the dust at high density. For example, the CS abundance falls by some five orders of magnitude

in the central region. When infall is included the situation is much different since dynamics allow the depleted zone to be replenished by infall of fresh material from the outer region with the result that the CS abundance decreases by only an order of magnitude. When these inner regions eventually become warm due to their proximity to a nascent central star, differences in abundance distributions will be more evident in the higher energy rotational transitions and will be prime targets for the new ALMA (Atacama Large Millimeter Array) interferometer in Chile.

### 1.5. Deuterium Fractionation

Deuterium is formed efficiently only in the Big Bang with an abundance relative to hydrogen which is sensitive to the baryon density, that is normal matter, in the Universe. Since this baryon density determines to a large extent the evolution of the Universe, measuring the deuterium abundance has been a matter of great importance to astrophysicists for almost 50 years. Such measurements are difficult to do because the deuterium equivalent of the hydrogen 21-cm line (the transition between the first-excited and lowest hyperfine split states of the 1s configuration) lies in a very unfavourable part of the radio spectrum while its UV Lyman-alpha line (2p-1s) can only be observed with space telescopes. Furthermore, the efficient extinction of UV radiation by dust means that absorption due to this line can only be studied in nearby regions, perhaps up to 3000 light years, from the Sun, a radius only about one-tenth of that of the Milky Way galaxy. Observations with the *FUSE* (Far Ultraviolet Satellite Explorer) satellite show that there is variation in the D/H ratio by about a factor of two, perhaps an indication that D is preferentially absorbed onto dust grains.<sup>64</sup> The local abundance ratio is in the region of  $(1-2)\times 10^{-5}$ , which we shall call the cosmic ratio, although it is likely to be smaller by a factor of a few than the ratio set in the Big Bang since D is — and has been — destroyed rather easily once incorporated into stars.

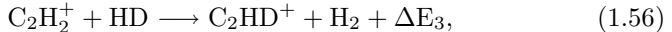
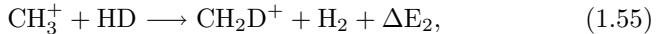
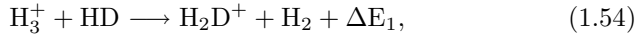
Despite the difficulty of observing atomic deuterium, it turns out that it is readily detected in interstellar molecules; 30 isotopologues of the 140 or so interstellar molecules have been observed (see Table 1.2). The initial detections were a surprise to radio astronomers because the intensity ratios implied abundances of deuterated molecules on the order of a few percent of their hydrogenated parents. Subsequently, astronomers detected the triply-deuterated molecules ND<sub>3</sub> and CD<sub>3</sub>OH, which have abundance ratios around  $10^{-4}$ , an enhancement of some 11 orders of magnitude over the statistical value — large even by astronomical standards. This enhancement, or fractionation, occurs because of small zero-point-energy differences between

Table 1.2. Deuterated interstellar molecules

HD	H <sub>2</sub> D <sup>+</sup>	D <sub>2</sub> H <sup>+</sup>	DCO <sup>+</sup>	N <sub>2</sub> D <sup>+</sup>	HDO
D <sub>2</sub> O	DCN	DNC	HDS	D <sub>2</sub> S	C <sub>2</sub> D
HDCO	D <sub>2</sub> CO	HDCS	D <sub>2</sub> CS	NH <sub>2</sub> D	NHD <sub>2</sub>
ND <sub>3</sub>	C <sub>4</sub> D	DC <sub>3</sub> N	DC <sub>5</sub> N	CH <sub>3</sub> OD	CH <sub>2</sub> DOH
CHD <sub>2</sub> OH	CD <sub>3</sub> OH	CH <sub>2</sub> DCN	CH <sub>3</sub> CCD	CH <sub>2</sub> DCCD	c-C <sub>3</sub> HD

reactants and products containing H and D.<sup>58,65,66</sup> These differences are negligible at room temperature but not at the temperatures of cold cores. In these regions the primary reservoirs of hydrogen and deuterium are H<sub>2</sub> and HD, respectively, with HD/H<sub>2</sub> = 2(D/H)<sub>cosmic</sub> ∼ 3 × 10<sup>-5</sup>.

The most important reactions which extract deuterium from HD involve ion-neutral isotope exchange reactions:



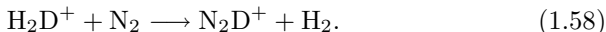
where the reaction exoergicities (defined as positive here), although small —  $\Delta E_1/k_B \sim 230$  K,  $\Delta E_2/k_B \sim 375$  K,  $\Delta E_3/k_B \sim 550$  K — are much larger than the temperatures of cold interstellar clouds. Hence at 10–20 K, the reverse reactions do not occur efficiently despite the large abundance of H<sub>2</sub>. As a result, the degree of fractionation, particularly in H<sub>2</sub>D<sup>+</sup>, can become large. Once formed, these deuterated ions can pass on their enhanced deuterium content to other species in chemical reactions.

It is instructive to consider the fractionation which arises in H<sub>2</sub>D<sup>+</sup>. In addition to the reverse of reaction (1.54), it can be destroyed by dissociative recombination with electrons and by reaction with neutral molecules, which we represent here by CO and HD. If one assumes steady-state, which is a reasonable approximation since the reactions are fast:

$$\frac{[\text{H}_2\text{D}^+]}{[\text{H}_3^+]} = \frac{k_{1f}}{k_{1r} + k_{1e}[e] + k_{\text{CO}}[\text{CO}] + k_{\text{HD}}[\text{HD}]} \frac{[\text{HD}]}{[\text{H}_2]}. \quad (1.57)$$

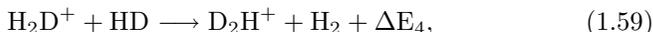
where [X] represents the fractional abundance of X relative to H<sub>2</sub>, k<sub>1f</sub> and k<sub>1r</sub> are the forward and reverse rate coefficients of reaction (1.54), k<sub>1e</sub> is the dissociative recombination rate coefficient of H<sub>2</sub>D<sup>+</sup>, and k<sub>CO</sub> and k<sub>HD</sub> are the rate coefficients for the reactions of H<sub>2</sub>D<sup>+</sup> with CO and HD. The ratio is a function of temperature because the rate coefficients are temperature dependent. For conditions typical of undepleted cold cores, k<sub>1r</sub> is negligible, as is dissociative recombination, the ion-neutral rate coefficients are roughly equal, and [CO] ∼ 10<sup>-4</sup> ∼ 10[HD]. Thus, [H<sub>2</sub>D<sup>+</sup>]/[H<sub>3</sub><sup>+</sup>] ∼ 10<sup>4</sup>

$[\text{HD}/\text{H}_2] \sim 0.1$ . This large fractionation in  $\text{H}_2\text{D}^+$  can be transmitted to other species through rapid deuteron transfer reactions, such as



If we assume that the transfer of the deuteron occurs statistically, i. e. in one-third of reactions, then this process leads to fractionation ratios of a few percent in  $\text{N}_2\text{D}^+$ , as observed in molecular clouds such as TMC-1. The  $\text{H}_2\text{D}^+$  ion is the dominant source of fractionation at 10 K as it is more abundant than either  $\text{CH}_2\text{D}^+$  or  $\text{C}_2\text{HD}^+$ . For clouds with temperatures larger than about 20 K, reaction with  $\text{H}_2$  (the reverse of reaction (1.54) dominates the denominator and the  $[\text{H}_2\text{D}^+]/[\text{H}_3^+]$  abundance ratio rapidly falls to its cosmic value. At these intermediate temperatures, fractionation by the hydrocarbon ions becomes important until 40–60 K when they too are destroyed by reaction with  $\text{H}_2$ . The reactivities of the hydrocarbon ions are different from that of  $\text{H}_2\text{D}^+$ , in particular the proton affinity of  $\text{N}_2$  is small so that  $\text{N}_2\text{D}^+$  can only be formed by  $\text{H}_2\text{D}^+$ . As such,  $\text{N}_2\text{D}^+$  is a tracer of cold, gas-phase chemistry.

We have seen that in high-density cold cores CO and other abundant molecules can be accreted onto dust grains. Once these molecules are depleted by an order of magnitude or so, reaction with HD now dominates the loss of  $\text{H}_2\text{D}^+$ , again assuming that dissociative recombination is unimportant. In this case  $\text{D}_3^+$  can be formed rapidly via:



where  $\Delta E_4/k_B \sim 187$  K and  $\Delta E_5/k_B \sim 159$  K. Since  $\text{D}_3^+$  is unreactive with HD, then it is possible that  $\text{D}_3^+$  can be more abundant than  $\text{H}_3^+$  and thus a more important deuteron donor than  $\text{H}_2\text{D}^+$ , not only because it is more abundant but also because it will transfer a deuteron on every reactive collision. This leads to very large fractionation in the gas phase.<sup>67</sup>

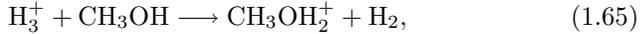
The construction of detailed chemical kinetic models describing deuterium chemistry is non-trivial and contains of necessity several approximations which are open to debate. For example, the reaction



has three deuterated equivalents:



Typically, one adopts the same total rate coefficient for each of the three reactive systems ( $C^+ + H_2O$ , HDO,  $D_2O$ ) but applies a statistical branching ratio to the products of the  $C^+ + HDO$  reaction, in this case 0.5. For more complex systems, additional approximations, often having to do with the preservation of functional groups within a reaction, are made. The proton transfer reaction:

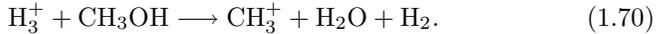


has four possible product channels when the neutral is singly-deuterated methanol:



One can include all four reactions in a reaction network or prescribe that the D atom must be retained in its functional group, thereby omitting the middle two reactions.

The number of reactions to be included in models of deuterium chemistry increases rapidly when one considers multiply-deuterated species. The reaction between  $H_3^+$  and  $CH_3OH$  actually has a second, dissociative, product channel in addition to proton transfer:



The  $H_3^+$  ion has three deuterated counterparts while methanol has seven. Thus there are now  $4 \times 8$  reactive collisions to be considered, each with multiple product channels. Each of the ions  $H_2D^+$  and  $D_2H^+$  has two possible product channels in each proton transfer reaction since they can transfer either a D or a H. If one applies the functional group rule, there are then 48 reactions involving proton transfer. Reaction (1.70) gives rise to even more possibilities because there are three products each containing hydrogen; even if the functional group rule is used to restrict possible channels there is a total of 64 reactions generated. Thus two reactions in a non-deuterated chemistry must be replaced by 112 in a fully deuterated model. Typically the inclusion of deuterium increases the number of reactions by a factor of four and species by a factor of two. Thus, as an example, a fairly modest interstellar model containing 199 species and 2717 reactions becomes one with 425 species and 13,848 reactions when fully deuterated using the functional group rule. Finally, there is some indication that in the dissociative recombination of deuterated ions, hydrogen atoms are lost preferentially over deuterium atoms so that statistical branching is not appropriate. Since

deuteron transfer is one of the major mechanisms by which deuterium is fractionated, such preferential retention of deuterium can have a large effect on the calculated abundances; unfortunately, very few systems have been studied experimentally.

Detailed models of deuterium chemistry have been made using realistic density profiles for static pre-stellar cloud cores.<sup>58</sup> These show that  $D_3^+$  becomes more abundant than  $H_3^+$  within a radial distance of 6000 AU from the centre of the cloud. At the very centre:

$$\frac{[D_3^+]}{[H_3^+]} \sim \frac{k_{1f}}{k_{3e}[e]} \frac{[HD]}{[H_2]} \sim 20, \quad (1.71)$$

where  $k_{3e}$  is the rate coefficient for the dissociative recombination of  $D_3^+$  with electrons. Subsequent support for this model has come from the detection of a rotational transition of para- $D_2H^+$  at 690 GHz with a similar intensity to the 372 GHz line of ortho- $H_2D^+$ . Observations at these frequencies are difficult due to water vapour absorption in the atmosphere and more accurate abundances in more sources will be a target for future instruments such as ALMA. The models also show that large fractionation occurs in multiply-deuterated species in these central, depleted regions within cold cores, and give  $[ND_3]/[NH_3] \sim 0.002$  and  $[NHD_2]/[NH_3] \sim 0.14$ , seemingly in good agreement with observation. These deuterated species are transient since they too will freeze out onto the dust particles with the implication that very highly fractionated sources will be difficult to detect in species like  $NHD_2$  since time scales are short. In essence, the only molecules predicted to be detectable via radio astronomy in the coldest, highest density cores are  $H_2D^+$  and  $D_2H^+$ ;<sup>68</sup> high-resolution spectral and spatial observations with ALMA will give unique dynamical and physical information on the late stages of low-mass star formation.

Figure 1.3 shows calculated fractionation ratios (abundance ratios of deuterated to normal species) for  $H_2D^+$ ,  $D_3^+$ , and  $D_2CO$  as functions of time for a homogeneous cloud of molecular hydrogen density  $10^6 \text{ cm}^{-3}$  and temperature 10 K. Results are shown both for no grain accretion (filled objects) and for grain accretion (unfilled objects). It can be seen that in the case of grain accretion, the fractionation ratios increase dramatically, especially for  $D_3^+$ , where the result approaches the approximation given in Eq. (1.71). Note also that the high  $D_2CO/H_2CO$  ratio seen for the case of grain accretion ends at a time of  $1 \times 10^5$  yr, when the species are almost totally accreted onto grain surfaces. At times later than this, the limiting case envisaged by Walmsley *et al.*<sup>68</sup> pertains in the absence of desorption mechanisms.

Although it is clear that deuterated cations observed in interstellar clouds are formed in gas-phase reactions, the situation is not so clear for

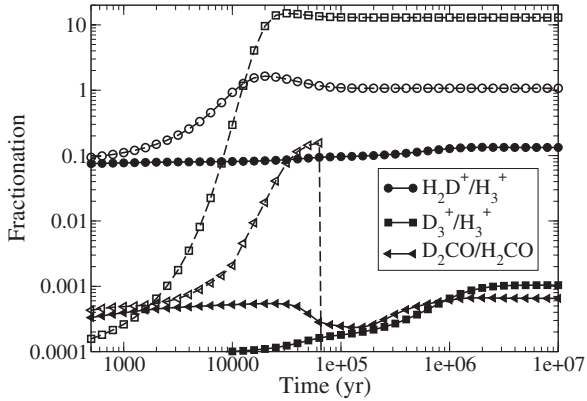


Fig. 1.3. Fractionation ratios plotted against time for a cloud with  $\text{H}_2$  density  $10^6 \text{ cm}^{-3}$  and temperature 10 K. Results with unfilled objects are for the case of grain accretion, whereas those with filled objects are for the case of no grain accretion. Calculation performed by Dr. Helen Roberts.

the neutral species. Consider highly depleted regions for which  $[\text{D}_3^+] \sim [\text{H}_3^+]$ . Dissociative recombination of these ions with electrons will lead to a high fractionation in atomic D. Since collisions with grains are rapid at high density, a large gas phase D/H ratio will be reflected in a large D/H ratio in the dust. As discussed in Sec. 1.3, it is believed that surface chemistry may play a substantial role in the synthesis of certain species, in particular  $\text{CH}_3\text{OH}$ , which is observed to be abundant in interstellar ices, and  $\text{H}_2\text{S}$ , for which no efficient gas-phase synthesis has been found at low temperature. Given the large abundance of CO which freezes out onto the grains it seems reasonable that addition and other reactions with H and D could lead to very large fractionation in  $\text{CH}_3\text{OH}$  and its intermediary  $\text{H}_2\text{CO}$ .<sup>45,46</sup> Indeed, some sources have  $[\text{D}_2\text{CO}]/[\text{H}_2\text{CO}] \sim 0.4$  and have a higher abundance of deuterated methanol, added over all isotopic forms, than normal methanol. As mentioned above, detailed models incorporating multiple deuteration can give rise to very large fractionation in the gas-phase in the innermost regions of the core. In fact, if one integrates the number density through the cloud to obtain column densities, which are derived from the radio telescope observations, a second difficulty arises, namely that the ratio of column densities can be much less than the local abundance ratios. For example, although  $[\text{D}_2\text{CO}]/[\text{H}_2\text{CO}]$  can be large in the central region of the core and close to that observed, the column density ratio is about an order of magnitude less than observed. This occurs because  $\text{H}_2\text{CO}$ , but not  $\text{D}_2\text{CO}$ , is formed readily in the outer region of the cloud and “dilutes” the ratio calculated for the inner region.

A further reason for thinking that grain surface chemistry might be responsible for creating large fractionation in some species comes from consideration of the structure of protonated neutrals. Consider formaldehyde as an example. Proton transfer leads to two structures, one, the less stable, protonated at the carbon end, the other protonated at the oxygen end, written  $\text{H}_2\text{COH}^+$ , an ion which has actually been detected in interstellar clouds. Thus when  $\text{H}_2\text{CO}$  is deuterated in the gas phase, the deuteron attaches preferentially to the oxygen atom. If the basic structure of the complex formed in the dissociative recombination with electrons is preserved, then the products are  $\text{H}_2\text{CO} + \text{D}$  and not  $\text{HDCO} + \text{H}$ . Isomerisation of the  $\text{H}_2\text{COD}$  intermediate may lead to  $\text{HDCO}$  but the efficiency is likely to be less than that assumed in models which ignore structure.<sup>69</sup> Similar arguments may be applied to the fractionation of the cyanopolyynes  $\text{HC}_3\text{N}$  and  $\text{HC}_5\text{N}$  and to methanol in the gas-phase. The situation for methanol is, in fact, somewhat more critical since the latest laboratory results show that only a few percent of dissociative recombinations of protonated methanol actually produce methanol.<sup>19</sup> The implication is that the methanol detected in cold clouds must have been formed on and released from cold grains. Since surfaces will be enriched in deuterium, large abundances of deuterated methanol are expected. The detailed processes by which a species like CO becomes hydrogenated or deuterated on the surface are discussed in Sec. 1.3.3.

In our discussion of deuteration we have implicitly assumed that all reactants are in their ground state and that rotational excitation does not affect the kinetics of the primary fractionation reactions. In fact this may not be the case. Since the  $J = 1$  (ortho) state of  $\text{H}_2$  lies 170 K above the  $J = 0$  (para) state, even a small fraction of  $\text{H}_2$  in  $J = 1$  will result in a faster destruction rate coefficient for  $\text{H}_2\text{D}^+$  than with  $J = 0$ . In highly depleted gas, destruction of  $\text{H}_2\text{D}^+$  via ortho- $\text{H}_2$  is more rapid than reaction with HD for a fractional abundance of ortho- $\text{H}_2$  greater than about one percent. Since the formation of  $\text{H}_2$  on interstellar dust is a highly exothermic process and the ejected molecule is likely to be superthermal internally, the initial ortho-para ratio is likely to be the high-temperature value of 3. This value is reduced through proton exchange reactions with  $\text{H}^+$  and  $\text{H}_3^+$  and reaches a steady-state value in the range  $10^{-3}$ – $10^{-4}$  compared with the equilibrium value of  $4 \times 10^{-7}$  at 10 K, on a time scale which may be longer than that of a particular cold core but shorter than that of molecular gas as a whole. Thus fractionation in  $\text{H}_3^+$  and related species may depend on the thermal and chemical history of the gas. The detailed processes and selection rules for the various processes which interconvert nuclear spin in  $\text{H}_2$ ,  $\text{H}_3^+$ ,  $\text{H}_2\text{D}^+$ ,  $\text{D}_2\text{H}^+$  and  $\text{D}_3^+$  are still a matter of debate<sup>70,71</sup> (see also chapter 3 by Gerlich) but it does appear that the very high fractionation ratios observed in highly

depleted cores may not all be the result of gas-phase reactions involving multiply-deuterated  $\text{H}_3^+$ .

## 1.6. Surface Chemistry: Mathematical Details and Gas-Grain Models

### 1.6.1. Rate Equations

The *kinetics* of  $\text{H}_2$  formation (and other surface reactions) via the Langmuir-Hinshelwood (diffusive) mechanism can be treated by rate equations, as in Eq. (1.52), or by stochastic methods.<sup>72</sup> There are two main objections to the former approach: it does not handle random-walk correctly and it fails in the limit of small numbers of reactive species. The latter objection is a far more serious one in the interstellar medium because dust particles are small, and the number of reactive atoms and radicals on their surfaces can be, on average, less than unity. Nevertheless, with rare exceptions, the few large models of interstellar chemistry that include surface processes as well as gas-phase chemistry do so via the rate equation approach, so we discuss it here. In the treatment below, we do not use the ordinary units of surface chemistry — areal concentrations or monolayers<sup>39</sup> — but instead refer to numbers of species on the mantle of an individual but average grain. Numbers can be converted to bulk concentrations, as used in Eq. (1.52), by multiplication by the grain number density  $n_d$ .

Consider two species, A and B, that can react on a grain surface via diffusion without activation energy. In the following discussion, we ignore the possibility that diffusion can occur by tunnelling. There are two reasons for this neglect: (1) careful experimental work<sup>40</sup> appears to exclude it for H atoms on olivine and amorphous carbon and (2) calculated potential barriers for physisorbed species tend to be very wide compared with chemical barriers (D. Woon 2007, private communication). If we follow the hopping of a single molecule of A from one site to another, the average (ensemble) probability of reaction with B after a hop to an adjacent binding site is given by the product of the hopping rate and the probability that the adjacent site is occupied by B. The hopping rate for species A  $k_{\text{hop,A}}$  ( $\text{s}^{-1}$ ) is given by the expression<sup>40</sup>

$$k_{\text{hop,A}} = \nu_0 \exp(-E_{\text{b,A}}/T) \quad (1.72)$$

where  $\nu_0$  is the “attempt” frequency (see also Eq. 1.53), typically taken as  $1\text{--}3 \times 10^{12} \text{ s}^{-1}$  for physisorbed species, and the energy barrier is written, as is common in astronomy, in units of K. The probability that B resides on an adjacent site is simply  $N(B)/N$ , where  $N(B)$  is the number of sites on

a grain occupied by B, and  $N$  is the total number of sites. With a standard site density of  $\approx 10^{15} \text{ cm}^{-2}$ , the number of sites on a grain of radius  $0.1 \mu\text{m}$  is  $\approx 10^6$ . Taking account of the fact that species B can also hop from site to site, we arrive at a rate law for the disappearance of A by reaction with B of

$$\frac{dN(A)}{dt} = -(k_{\text{hop,A}} + k_{\text{hop,B}})N(A)N(B)/N. \quad (1.73)$$

Equation (1.73) can be rewritten as

$$\frac{dN(A)}{dt} = -(k_{\text{diff,A}} + k_{\text{diff,B}})N(A)N(B) = -k_{\text{AB}}N(A)N(B), \quad (1.74)$$

where the first-order rate coefficients for diffusion are loosely defined as the hopping rates over a number of sites equivalent to the total number of sites on the dust particle, although, of course, the process of “back diffusion” means that the total grain is not seen by the diffusing particle in only  $N$  moves. If atomic hydrogen is a reactant, its uniquely low barrier against diffusion means that the diffusion of a heavier reactant need not be considered. Indeed, for cores at 10 K, the only major reactant that moves on surfaces rapidly is atomic hydrogen. It is important to reiterate that although  $\text{H}_2$  is the dominant form of hydrogen in dense clouds, there can be sufficient atomic hydrogen to render it an important surface reactant.

If there is chemical activation energy  $E_A$  in addition to the barrier to diffusion, two revisions of Eq. (1.74) have been suggested.<sup>73</sup> The simpler is to add either a tunnelling probability or hopping probability (Boltzmann factor), whichever is greater, as a simple factor, labelled  $\kappa$ , so that the rate coefficient  $k_{\text{AB}}$  is multiplied by  $\kappa$ . In the case of hopping,

$$\kappa = \exp(-E_A/T), \quad (1.75)$$

whereas in the case of tunnelling,

$$\kappa = P_{\text{tunn}}. \quad (1.76)$$

For a rectangular potential of width  $a$ ,

$$P_{\text{tunn}} = \exp[-2(a/\hbar)\sqrt{(2\mu E_A)}], \quad (1.77)$$

where  $\mu$  is the reduced mass of the A-B system.

The more complex revision is to consider diffusive hopping from one site to another as competitive with tunnelling through or hopping over the activation energy barrier. If we assume that tunnelling under the activation energy barrier dominates hopping over it, the additional factor  $\kappa$  can be written in the steady-state limit as

$$\kappa = \frac{k_{\text{tunn}}}{k_{\text{tunn}} + k_{\text{hop,A}} + k_{\text{hop,B}}}, \quad (1.78)$$

where

$$k_{\text{tunn}} = \nu_0 \times P_{\text{tunn}}. \quad (1.79)$$

In this case, if the tunnelling rate exceeds the two diffusive hopping rates, the activation barrier does *not* impede the rate of reaction! On the other hand, if the tunnelling rate is much slower than the diffusive hopping rates, the more complex expression for  $\kappa$  reduces to

$$\kappa \approx \frac{k_{\text{tunn}}}{k_{\text{hop,A}} + k_{\text{hop,B}}}, \quad (1.80)$$

and the rate coefficient  $k_{\text{AB}}$  becomes

$$k_{\text{AB}} \approx k_{\text{tunn}}/N, \quad (1.81)$$

which is formally independent of the rate of diffusion. Nevertheless, the difference between the result of Eq. (1.81) and the simple approach with tunnelling is often minimal. The microscopic stochastic approach discussed below suggests that the competitive mechanism is the correct one,<sup>74</sup> but this view is not universal.<sup>75</sup>

To place species A into a chemical model with both gas-phase and surface processes also requires inclusion of adsorption and desorption. Adsorption onto a single grain follows a simple bimolecular rate law of the type

$$\frac{dN(A)}{dt} = S_A v_A \sigma n(A), \quad (1.82)$$

where  $n(A)$  is the gas-phase density of A and the other parameters have been defined in the discussion following Eq. (1.51). If one wishes to estimate a rate for the bulk adsorption of A, one must also multiply both sides of Eq. (1.82) by the dust grain density.

Thermal desorption (evaporation) can be handled by the so-called first-order Polanyi-Wigner equation, which for an individual grain takes the form<sup>39</sup>

$$\frac{dN(A)}{dt} = -k_{\text{te,A}} N(A), \quad (1.83)$$

where  $k_{\text{te}}$  is defined in Eq. (1.53). Experimentalists often report evaporation as a zeroth-order process if many monolayers are involved and no net change is detected. There is even a second-order Polanyi-Wigner equation, for situations in which desorption follows reaction.<sup>39,40</sup> Finally, in cold interstellar cloud cores, little evaporation takes place for any species more strongly bound than H and H<sub>2</sub>, so that non-thermal desorption processes must be considered. Mechanisms based on the exothermicity of surface chemical

reactions, cosmic ray bombardment, photon bombardment, and grain-grain collisions have been included (see Sec. 1.4.2). A recent experiment shows a measurable rate of photodesorption for the case of pure CO ice bombarded with far-UV photons.<sup>52</sup>

In addition to the problems already mentioned, the rate equation treatment makes no distinctions about where the adsorbates are located; they can be in any monolayer of the mantle (and the number of monolayers in an icy mantle can range up to several hundred) and they can be in any site of a monolayer. In other words, the details of reactions are averaged over vertical and horizontal features. The vertical problem can be partially removed by restricting processes to the topmost monolayer, although in porous systems this restriction is not obviously true.

### 1.6.2. *Stochastic Approaches*

The assumptions and problems inherent in the rate equation approach can be removed by assorted stochastic treatments, although these typically involve far more computer time and are difficult to couple with gas-phase rate equations.<sup>72</sup> The problem of average adsorbate abundances that are less than unity on individual dust particles can be removed by so-called macroscopic stochastic methods, which take both the discrete numbers of adsorbates per grain and their fluctuations into account. The methods involve either a Monte Carlo treatment, in which random numbers are chosen to determine what process occurs during a time interval, or a master equation approach, which contains differential equations as in the rate-equation treatment. Instead of solving for the average number of adsorbates per grain, however, these methods solve for the probability as a function of time that a certain number of adsorbates are present.<sup>76</sup> For example, one replaces the one differential equation for  $N(A)$  above, with a series of equations for  $P_n(A)$ , the probability that  $n$  atoms of A are present on a grain. Unfortunately, although such a treatment increases the number of equations, it does not represent the full complexity of the method because probabilities of different species are correlated; that is, one must solve for the joint probability of, say,  $n$  atoms of H,  $m$  atoms of O,  $p$  atoms of C, etc. In order to accomplish this goal, it is useful to divide the set of different adsorbates into reactive atoms and radicals, which never build up a large surface abundance, and inert or weakly reactive species, such as CO, which can achieve large abundances of more than 1–10 monolayers. The atoms/radicals require a stochastic treatment whereas the chemistry of the species with large abundances can be treated by rate equations. Nevertheless, there are still convergence problems if average abundances of reactive species exceed unity, and as of the present the macroscopic master

equation method has only been used in models with small networks of surface reactions. A new approximation to the master equation treatment may be sufficiently efficient to allow its usage with large models under a wide range of conditions.<sup>75</sup>

A more detailed treatment of surface chemistry has recently been reported; this method, known as the continuous-time random-walk approach, is a Monte Carlo treatment in which random walk is treated exactly and the details of local surface morphology included.<sup>42,72,77</sup> The grain surface is divided into a two-dimensional lattice of sites, corresponding to potential minima. One can start with a flat surface, in which all sites are identical, or a rough surface, in which all sorts of imperfections cause local changes in the potential. Rough surfaces with given percentages of irregularities can themselves be obtained by Monte Carlo methods. To perform the calculation, one considers adsorption, desorption, hopping, and possible tunnelling under activation energy barriers to be Markovian (memory-less) events, in which the time interval between two consecutive events follows a Poisson distribution of the type

$$f(t) = k \exp(-kt), \quad (1.84)$$

where  $k$  is a first-order rate coefficient, such as that given for diffusive hopping in Eq. (1.72). Once the calculation commences, random numbers are called to determine the time interval for each process, and this is added to the current time. Then, as the clock moves forward, the events are allowed to occur at the appropriate time, when, in addition, the next interval for the process is determined by the choice of another random number. The hopping of all individual adsorbates can be followed, and activation-less reactions occur if two adsorbates occupy the same site. If there is activation energy, the competition between hopping and tunnelling through an activation energy barrier can also be followed. If, for any adsorbate, the time interval for desorption is shorter than that for hopping, then the species desorbs at the appropriate time.

Although the method has been used to study the formation of  $\text{H}_2$  on surfaces pertaining to diffuse clouds, and the formation and morphology of ices grown in cold cores,<sup>42,74</sup> it has proven very difficult to use it simultaneously with a gas-phase chemistry that is treated adequately by rate equations. The basic problem appears to be that the subroutines used to solve the coupled differential equations for gas-phase kinetics choose time intervals that are different from the random time intervals chosen from the Poisson distributions. A preliminary paper that reports an attempt to couple the two methods by a linearization procedure has just appeared in the literature. Even with this approximation, only a small number of surface reactions can be treated simultaneously.<sup>77</sup>

### 1.6.3. Gas-Grain Models of Cold Cores

We have previously focused attention on purely gas-phase chemical models, gas-phase models with accretion onto grains, and gas-phase models with both accretion and desorption. Gas-grain models, such as that of Aikawa *et al.*<sup>62</sup> briefly mentioned above, differ from these models in that they include surface chemistry. For models with large numbers of surface reactions, either the simple rate equation treatment is used, or the rate coefficients  $k_{AB}$  (see Eq. (1.74)) are modified in a semi-empirical manner to handle fractional average adsorbate abundances to an extent. The so-called “modified rate treatment” has been tested against stochastic methods in small systems of equations.<sup>72</sup>

For a non-collapsing cold interstellar core such as TMC-1, we have already shown that the time scale against striking a grain is  $\approx 3 \times 10^5$  yr, which is equivalent to the gas-phase chemical time scale to reach early-time abundances. During this time, the major chemical processes that occur on granular surfaces in a gas-grain chemical model are the production of mantle species from the initial constituents of the gas and from species formed early in the gas. If the initial gas is assumed to be atomic, except for the high abundance of  $H_2$ , the most important early process is the formation of water ice from oxygen and hydrogen atoms colliding with and sticking to dust particles. As the gas-phase abundance of CO increases towards the end of the first  $10^5$  yr of the existence of the core and its accretion rate also increases, the rate of its hydrogenation into surface formaldehyde and methanol proceeds until significant abundances of these surface species exist. Within a decade of time later, however, the gas-phase becomes strongly depleted of heavy species, as in simple accretion models, in the absence of desorption (see Fig. 1.2). Unless non-thermal desorption mechanisms exist, the results of gas-grain models for gas-phase and mantle abundances can only be compared with observation for a short period of time during which a substantial mantle has developed and the gas-phase has only lost a small fraction of its heavy material. If, however, non-thermal desorption mechanisms are included, this period of time can be extended.

Let us briefly consider a very recent model of the gas-grain chemistry of a cold interstellar core, in which several mechanisms for non-thermal desorption are considered, including cosmic-ray-induced desorption, “indirect” photodesorption, and exothermicity-induced desorption.<sup>6</sup> Of these, the dominant process is the third. Most surface reactions in these models are associative in nature, with the grain acting in part as a third body to remove enough energy to stabilise the single product. Since these reaction exothermicities are typically much larger than physisorption binding energies, it is entirely possible that sufficient energy can be directed into the physisorption bond to break it. In the absence of much experimental information on

the efficiency of this process, one can utilise unimolecular rate theory to estimate the probability that a surface association reaction can lead to the ejection of the product molecule. With the crude RRK approach, Garrod *et al.*<sup>6</sup> estimated that the fraction  $f$  of desorbed products in a competition with loss of energy to the grain is given by the expression

$$f = \frac{aP}{1 + aP}, \quad (1.85)$$

where  $a$  is treated as a parameter, and  $P$  is the RRK expression for the probability that a greater amount of energy than needed for desorption is present in the adsorbate-surface bond. The standard expression for  $P$  is given by

$$P = [1 - E_D/E_{\text{exo}}]^{s-1}, \quad (1.86)$$

where  $E_D$  is the energy associated with the bond between the surface and the adsorbed molecule,  $E_{\text{exo}}$  is the reaction exothermicity and  $s$  is the number of vibrational modes in the molecule-surface bond system. Note that  $a = 1$  yields the pure RRK treatment.

Although there is no direct photodesorption in the model, there is photodissociation of surface adsorbates, and such photodissociation produces radical and atomic fragments, which can recombine with other atoms and radicals, leading to the possibility of desorption via exothermic reactions. The final mechanism considers the temperature increase in a grain following attack by a cosmic ray particle, and follows the rate of evaporation as the grain cools.

Use of this gas-grain model seems to lengthen the time of best agreement with gas-phase observation for the cold cores L134N and TMC-1 up to perhaps  $2\text{--}3 \times 10^6$  yr, at which time the fraction of molecules with abundances predicted to be within an order-of-magnitude of the observed abundances is 0.80–0.85 for L134N and 0.65–0.70 for TMC-1 (see a similar effect in the accretion-desorption model of Willacy & Millar<sup>56</sup>). The dependence on time is rather flat, however, especially for L134N. Values of the parameter  $a$  of 0.01, 0.03, and 0.10 were used and yield results statistically insignificant from each other; a value of  $a = 0$  yields worse results. One important gas-phase molecule produced sufficiently in this model but not in purely gas-phase approaches is methanol, which comes off the grains during its exothermic formation.

As regards the agreement with mantle abundances at these times, the cold core sources have not been studied in detail in infrared absorption, so it is best to use the well-studied source Elias 16, which lies near TMC-1, astronomically speaking. The level of agreement can best be described as moderate, with the high abundance of water ice securely reproduced, but the abundances of CO and CO<sub>2</sub> ice underproduced and the abundances of NH<sub>3</sub> and CH<sub>4</sub> ice overproduced. It should be noted that smaller but

stochastic models, in which only surface chemistry is considered, with nearly constant fluxes of gas-phase material upon the grains, can achieve much better agreement for the mantle abundances.<sup>77</sup>

What happens as the age of the cold core becomes considerably greater than  $10^6$  yr? It is instructive to follow the dominant form of carbon. First, a high flux of gaseous CO is adsorbed onto grains and reacts to form sufficient surface methanol so that it starts to dominate, although by  $10^7$  yr the dominant form of carbon shifts to methane ice via a complex sequence of reaction, non-thermal desorption, and accretion. Finally, at very long times of  $10^8$  yr or so, the dominant form of carbon is a mixture of mantle hydrocarbons more complex than methane. Meanwhile, the non-thermal desorption processes are sufficiently efficient that sizeable portions of gas-phase material remain. For example, gas-phase CO achieves a nearly steady-state fractional abundance of  $10^{-6}$  and ammonia of  $10^{-7}$ . Of course, such long times may have little physical meaning since collapse leading to star formation through stages such as pre-stellar cores and hot cores will probably have already begun.

A late-time chemistry may have been discovered recently in a different context in the star-forming region L1527, in which a general temperature of  $\approx 30$  K pertains in the vicinity of the protostar.<sup>78</sup> In this protostellar source, the observed molecules strongly resemble those in TMC-1, and include unsaturated radical hydrocarbons and cyanopolynes. What chemistry can lead to such species at such a late stage of stellar evolution following the pre-stellar core stage where most heavy molecules deplete onto cold 10 K grains? There are two possibilities. We may be dealing with gas that did not accrete onto grains, perhaps from the outer regions of pre-stellar cores. Or, the TMC-1-like molecules originate from the evaporation of mantle material. Unlike the case of hot cores, where the temperature has already risen to 200–300 K in the vicinity of star formation, here a temperature of only 30 K has been achieved. At this temperature, methane and CO ice desorb efficiently into the gas. Of the two, methane is the likely precursor of the TMC-1 carbon-chain molecules, starting with reactions such as Eq. (1.34). Is the 30 K material gradually heating up to form a hot core? Or is 30 K the asymptotic temperature after the heat-up phase? At present, we do not know the answers to these questions. Indeed, despite more than 35 years of active investigation in astrochemistry, there still remain many unanswered questions in this exciting interdisciplinary area of science.

## Acknowledgement

Astrophysics at QUB is supported by a grant from the Science and Technology Facilities Council (UK). EH acknowledges support for his research program in astrochemistry by the National Science Foundation (USA).

## References

1. Lis D, Blake GA, Herbst E. (eds). (2006) *Astrochemistry: Recent Successes and Current Challenges*, Cambridge University Press, Cambridge.
2. Tielens AGGM. (2005) *The Physics and Chemistry of the Interstellar Medium*, Cambridge University Press, Cambridge.
3. Woon DE. (2006) <http://www.astrochymist.org/>
4. Whittet DCB. (2002) *Dust in the Galactic Environment*, Institute of Physics, London.
5. Williams D, Brown WA, Price SD, Rawlings JMC, Viti S. (2007) Molecules, ices and astronomy. *Ast. & Geophys.* **48**: 1-25-1.34.
6. Garrod RT, Wakelam V, Herbst E. (2007) Nonthermal desorption from interstellar dust grains via exothermic surface reactions. *Astron. & Astrophys.* **467**: 1103–1115.
7. Herbst E. (2005) Chemistry of Star-Forming Regions. *J. Phys. Chem.* **109**: 4017–4029.
8. Le Petit F, Roueff E, Herbst E. (2004)  $\text{H}_3^+$  and other species in the diffuse cloud towards  $\zeta$  Persei: A new detailed model. *Astron. & Astrophys.* **417**: 993–1002.
9. Oka T. (2006) Introductory remarks. *Phil. Trans. R. Soc. A* **364**: 2847–2854.
10. Anicich VG. (2003) *An index of the literature for bimolecular gas-phase cation-molecule reaction kinetics*. Jet Propulsion Laboratory (JPL-Publ-03-19).
11. Herbst E. (2006) Gas Phase Reactions. In GWF Drake (ed.) *Handbook of Atomic, Molecular, and Optical Physics*, pp. 561–573, Springer Verlag, Leipzig.
12. Herbst E, Leung CM. (1986) Effects of Large Rate Coefficients for Ion-Polar Neutral Reactions on Chemical Models of Dense Interstellar Clouds. *Astrophys. J.* **310**: 378–382.
13. Smith D, Adams NG. (1987) The selected ion flow tube (SIFT): studies of ion-neutral reactions. *Adv. Atom. Mol. Phys.* **24**: 1–49.
14. Huntress WT Jr. (1977) Laboratory studies of bimolecular reactions of positive ions in interstellar clouds, in comets, and in planetary atmospheres of reducing composition. *Astrophys. J. Suppl.* **33**: 495–514.
15. Woodall J, Agúndez M, Markwick-Kemper AJ, Millar TJ. (2007) The UMIST database for astrochemistry 2006. *Astron. & Astrophys.* **466**: 1197–1204. See also <http://www.udfa.net>.
16. Florescu-Mitchell AI, Mitchell JBA. (2006) Dissociative recombination. *Physics Reports* **430**: 277–374.
17. Weston Jr RE, Schwarz HA. (1972) *Chemical Kinetics*. Prentice-Hall, Englewood Cliffs.
18. Herd CR, Adams NG, Smith D. (1990) OH Production in the dissociative recombination of  $\text{H}_3\text{O}^+$ ,  $\text{HCO}_2^+$ , and  $\text{N}_2\text{OH}^+$  — Comparison with theory and interstellar implications. *Astrophys. J.* **349**: 388–392.
19. Geppert WD, Hamberg M, Thomas RD, Österdahl F, Hellberg F, Zhaunerchik V, Ehlerding A, Millar TJ, Roberts H, Semaniak J, af Ugglas M,

- Källberg A, Simonsson A, Kaminska M, Larsson M. (2006) Dissociative recombination of protonated methanol. *Faraday Discussions* **133**: 177–190.
20. Jensen MJ, Bilodeau RC, Safvan CP, Seiersen K, Andersen LH, Pedersen HB, Heber O. (2000) Dissociative Recombination of  $\text{H}_3\text{O}^+$ ,  $\text{HD}_2\text{O}^+$ , and  $\text{D}_3\text{O}^+$ . *Astrophys. J.* **543**: 764–774.
21. Semaniak J, Minaev BF, Derkach AM, Hellberg F, Neau A, Rosen S, Thomas R, Larsson M, Danared H, Paäl A, af Ugglas M. (2001) Dissociative Recombination of  $\text{HCNH}^+$ : Absolute Cross Sections and Branching Ratios. *Astrophys. J. Suppl.* **135**: 275–283.
22. Smith IWM, Herbst E, Chang Q. (2004) Rapid neutral-neutral reactions at low temperatures: a new network and first results for TMC-1. *Mon. Not. R. Astron. Soc.* **350**: 323–330. See also [www.physics.ohio-state.edu/~eric](http://www.physics.ohio-state.edu/~eric).
23. Carty D, Goddard A, Köhler SPK, Sims IR, Smith IWM. (2006) Kinetics of the Radical-Radical Reaction,  $\text{O}(^3\text{P}_J) + \text{OH}(X\ ^2\Pi_\Omega) \rightarrow \text{O}_2 + \text{H}$ , at Temperatures Down to 39 K. *J. Phys. Chem. A* **110**: 3101–3109.
24. Xu C, Xie D, Honvault P, Lin SY, Guo H. (2007) Rate constant for  $\text{OH}(^2\Pi) + \text{O}(^3\text{P}) \rightarrow \text{H}(^2\text{S}) + \text{O}_2(^3\Sigma_g^-)$  reaction on an improved *ab initio* potential energy surface and implications for the interstellar oxygen problem. *J. Chem. Phys.* **127**: 024304.
25. Sims IR. (2006) Experimental Investigation of Neutral-Neutral Reactions and Energy Transfer at Low Temperatures. In Lis D, Blake GA, Herbst E. (eds). *Astrochemistry: Recent Successes and Current Challenges*, pp. 97–108. Cambridge University Press, Cambridge.
26. Smith IWM, Sage AM, Donahue NM, Herbst E, Quan D. (2006) The temperature-dependence of rapid low temperature reactions: experiment, understanding and prediction. *Faraday Discuss.* **133**: 137–156.
27. Sabbah H, Bienner L, Sims IR, Georgievskii, Klippenstein SJ, Smith IWM. (2007) Understanding Reactivity at Very Low Temperatures: The Reactions of Oxygen Atoms with Alkenes. *Science* **317**: 102–105.
28. Gerlich D, Horning S. (1992) Experimental Investigations of Radiative Association Processes as Related to Interstellar Chemistry. *Chem. Rev.* **92**: 1509–1539.
29. Bates DR, Herbst E. (1988) Radiative Association. In TJ Millar & DA Williams (eds). *Rate Coefficients in Astrochemistry*, pp. 17–40, Kluwer Academic Publishers, Dordrecht.
30. Herbst E. (1985) An Update of and Suggested Increase in Calculated Radiative Association Rate Coefficients. *Astrophys. J.* **291**: 226–229.
31. Chastaing D, Le Picard SD, Sims IR, Smith IWM. (2001) Rate coefficients for the reactions of  $\text{C}(^3\text{P}_J)$  atoms with  $\text{C}_2\text{H}_2$ ,  $\text{C}_2\text{H}_4$ ,  $\text{CH}_3\text{CCH}$  and  $\text{H}_2\text{CCCH}_2$  at temperatures down to 15 K. *Astron. & Astrophys.* **365**: 241–247.
32. Cartechini L, Bergeat A, Capozza G, Casavecchia P, Volpi GG, Geppert WD, Naulin C, Costes M. (2002) Dynamics of the  $\text{C} + \text{C}_2\text{H}_2$  reaction from differential and integral cross-section measurements in crossed-beam experiments. *J. Chem. Phys.* **116**: 5603–5611.
33. Herbst E. (1981) Can negative molecular ions be detected in dense interstellar clouds? *Nature* **289**: 656–657.

34. Petrie S, Herbst E. (1997) Some interstellar reactions involving electrons and neutral species: Attachment and isomerization. *Astrophys. J.* **491**: 210–215.
35. Güthe F, Tulej M, Pachkov MV, Maier JP. (2001) Photodetachment Spectrum of  $l\text{-C}_3\text{H}_2\text{H}^-$ : The Role of Dipole Bound States for Electron Attachment in Interstellar Clouds. *Astrophys. J.* **555**: 466–471.
36. Millar TJ, Walsh C, Cordiner MA, Ní Chuimín R, Herbst E. (2007) Hydrocarbon Anions in Interstellar Clouds and Circumstellar Envelopes. *Astrophys. J.* **662**: L87–L90.
37. McCarthy MC, Gottlieb CA, Gupta H, Thaddeus P. (2006) Laboratory and Astronomical Identification of the Negative Molecular Ion  $\text{C}_6\text{H}^-$ . *Astrophys. J.* **652**: L141–L144.
38. Remijan AJ, Hollis JM, Lovas FJ, Cordiner MA, Millar TJ, Markwick-Kemper AJ, Jewell PR. (2007) Detection of  $\text{C}_8\text{H}^-$  and Comparison with  $\text{C}_8\text{H}$  toward IRC + 10216. *Astrophys. J.* **664**: L47–L50.
39. Kolasinski K. (2002) *Surface Science. Foundations of Catalysis and Nanoscience*, John Wiley & Sons, Ltd., West Sussex, UK.
40. Katz N, Furman I, Biham O, Pirronello V, Vidali G. (1999) Molecular Hydrogen Formation on Astrophysically Relevant Surfaces. *Astrophys. J.* **522**: 305–312.
41. Peretz HB, Lederhendler A, Biham O, Vidali G, Li L, Swords S, Congiu E, Roser J, Manicó G, Brucato JR, Pirronello V. (2007) Molecular Hydrogen Formation on Amorphous Silicates under Interstellar Conditions *Astrophys. J.* **661**: L163–L166.
42. Cuppen H, Morata O, Herbst E. (2005) Monte Carlo simulations of  $\text{H}_2$  formation on stochastically heated grains. *Mon. Not. R. Astron. Soc.* **367**: 1757–1765.
43. Hornekaer L, Baurichter A, Petrunin VV, Field D, Luntz AC. (2003) Importance of Surface Morphology in Interstellar  $\text{H}_2$  Formation. *Science* **302**: 1943–1946.
44. Tiné S, Williams DA, Clary DC, Farebrother AJ, Fisher AJ, Meijer AJHM, Rawlings JMC, David CJ. (2003) Observational Indicators of Formation Excitation of  $\text{H}_2$ . *Astrophys. & Sp. Sci.* **288**: 377–389.
45. Watanabe N, Nagaoka A, Shiraki T, Kouchi A. (2004) Hydrogenation of CO on Pure Solid CO and CO- $\text{H}_2\text{O}$  Mixed Ice. *Astrophys. J.* **616**: 638–642.
46. Nagaoka A, Watanabe N, Kouchi A. (2005) H-D Substitution in Interstellar Solid Methanol: A Key Route for D Enrichment. *Astrophys. J.* **624**: L29–L32.
47. See the URL [massey.dur.ac.uk/drf/protostellar](http://massey.dur.ac.uk/drf/protostellar).
48. Wakelam V, Herbst E, Selsis F. (2006) The effect of uncertainties on chemical models of dark clouds. *Astron. & Astrophys.* **451**: 551–562.
49. Landau LD, Lifshitz EM. (1960) *Course of Theoretical Physics. Vol. 1, Mechanics*. Pergamon Press, New York.
50. Collings MP, Anderson MA, Chen R, Dever JW, Viti S, Williams DA, McCoustra MRS. (2004) A laboratory survey of the thermal desorption of astrophysically relevant molecules. *Mon. Not. R. Astron. Soc.* **354**: 1133–1140.

51. Bringa EM, Johnson RE. (2004) A New Model for Cosmic-Ray Ion Erosion of Volatiles from Grains in the Interstellar Medium. *Astrophys. J.* **603**: 159–164.
52. Öberg KI, Fuchs GW, Awad Z, Fraser HJ, Schlemmer S, van Dishoeck EF, Linnartz H. (2007) Photodesorption of CO Ice. *Astrophys. J.* **662**: L23–L26.
53. Gredel R, Lepp S, Dalgarno A, Herbst E. (1989) Cosmic-ray-induced Photodissociation and Photoionization Rates of Interstellar Molecules. *Astrophys. J.* **347**: 289–293.
54. Willacy K, Williams DA. (1993) Desorption processes in molecular clouds — Quasi-steady-state chemistry. *Mon. Not. R. Astron. Soc.* **260**: 635–642.
55. Shalabiea OM, Greenberg JM. (1994) Two key processes in dust/gas chemical modelling: photoprocessing of grain mantles and explosive desorption. *Astron. & Astrophys.* **290**: 266–278.
56. Willacy K, Millar TJ. (1998) Desorption processes and the deuterium fractionation in molecular clouds. *Mon. Not. R. Astron. Soc.* **298**: 562–568.
57. Ward-Thompson D, Motte F, Andre P. (1999) The initial conditions of isolated star formation - III. Millimetre continuum mapping of pre-stellar cores. *Mon. Not. R. Astron. Soc.* **305**: 143–150.
58. Roberts H, Herbst E, Millar TJ. (2004) The chemistry of multiply deuterated species in cold, dense interstellar cores. *Astron. & Astrophys.* **424**: 905–917.
59. Bisschop SE, Fraser HJ, Öberg KI, van Dishoeck ER, Schlemmer S. (2006) Desorption rates and sticking coefficients for CO and N<sub>2</sub> interstellar ices. *Astron. & Astrophys.* **449**: 1297–1309.
60. Tafalla M, Myers PC, Caselli P, Walmsley CM, Comito C. (2002) Systematic Molecular Differentiation in Starless Cores. *Astrophys. J.* **569**: 815–835.
61. Lee JE, Bergin EA, Evans II NJ. (2004) Evolution of Chemistry and Molecular Line Profiles during Protostellar Collapse. *Astrophys. J.* **617**: 360–383.
62. Aikawa Y, Herbst E, Roberts H, Caselli P. (2005) Molecular Evolution in Collapsing Prestellar Cores. III. Contraction of a Bonnor-Ebert Sphere. *Astrophys. J.* **620**: 330–346.
63. Lee JE, Evans II NJ, Bergin EA. (2005) Comparisons of an Evolutionary Chemical Model with Other Models. *Astrophys. J.* **631**: 351–360.
64. Linsky J + 17 co-authors. (2006) What is the Total Deuterium Abundance in the Local Galactic Disk? *Astrophys. J.* **647**: 1106–1124.
65. Roberts H, Millar TJ. (2000) Modelling of deuterium chemistry and its application to molecular clouds. *Astron. & Astrophys.* **361**: 388–398.
66. Roberts H, Millar TJ. (2006) Deuterated H<sub>3</sub><sup>+</sup> as a probe of isotope fractionation in star-forming regions. *Phil. Trans. R. Soc. A* **364**: 3063–3080.
67. Roberts H, Herbst E, Millar TJ. (2003) Enhanced Deuterium Fractionation in Dense Interstellar Cores Resulting From Multiply Deuterated H<sub>3</sub><sup>+</sup>. *Astrophys. J.* **591**: L41–L44.
68. Walmsley CM, Flower DR, Pineau des Forêts G. (2004) Complete depletion in prestellar cores. *Astron. & Astrophys.* **418**: 1035–1043.
69. Osamura Y, Roberts H, Herbst E. (2005) The Gas-Phase Deuterium Fractionation of Formaldehyde. *Astrophys. J.* **621**: 348–358.

70. Uy D, Cordonnier M, Oka T. (1997) Observation of Ortho-Para  $\text{H}_3^+$  Selection Rules in Plasma Chemistry. *Phys. Rev. Lett.* **78**: 3844–3847.
71. Gerlich D, Windisch F, Hlavenka P, Plasil R, Glosik J. (2006) Dynamical constraints and nuclear spin caused restrictions in  $\text{H}_m\text{D}_n^+$  collision systems. *Phil. Trans. R. Soc. A* **364**: 3007–3034
72. Herbst E, Chang Q, Cuppen H. (2005) Chemistry on interstellar grains. *J. Phys.: Conf. Ser.* **6**: 18–35.
73. Awad Z, Chigai T, Kimura Y, Shalabiea OM, Yamamoto T. (2005) New Rate Constants of Hydrogenation of CO on  $\text{H}_2\text{O}$ -CO Ice Surfaces. *Astrophys. J.* **626**: 262–271.
74. Cuppen HM, Herbst E. (2007) Simulation of the Formation and Morphology of Ice Mantles on Interstellar Grains. *Astrophys. J.* **668**: 294–309.
75. Barzel B, Biham O. (2007) Efficient Simulations of Interstellar Gas-Grain Chemistry Using Moment Equations. *Astrophys. J.* **658**: L37–L40.
76. Biham O, Furman I, Pirronello V, Vidali G. (2001) Master Equation for Hydrogen Recombination on Grain Surfaces. *Astrophys. J.* **553**: 595–603.
77. Chang Q, Cuppen HM, Herbst E. (2007) Gas-grain chemistry in cold interstellar cloud cores with a microscopic Monte Carlo approach to surface chemistry. *Astron. & Astrophys.* **469**: 973–983.
78. Sakai N, Sakai T, Hirota T, Yamamoto S. (2008) Abundant Carbon-Chain Molecules toward Low-Mass Protostar IRAS04368 + 2557 in L1527. *Astrophys. J.* **672**: 371–381.